THERMAL ANALYSIS OF FILLER REINFORCED POLYMERIC COMPOSITES

by

Mahesh Devidas Ghadge

A thesis submitted to the faculty of
The University of North Carolina at Charlotte
in partial fulfillment of the requirements
for the degree of Master of Science in
Mechanical Engineering

Charlotte

2017

Approved by:

_____
Dr. Alireza Tabarraei

_____
Dr. Gloria Elliott

_____
Dr. Vincent Ogunro

ABSTRACT

MAHESH DEVIDAS GHADGE. Thermal analysis of filler reinforced polymeric composites. (Under the direction of DR. ALIREZA TABARRAEI)

Improving heat dissipating property of composite materials is becoming increasingly important in domains ranging from the automotive industry, electronic devices to aeronautical industry. Effective heat dissipation is required especially in aircraft and racing tires to guarantee high performance and good service life [1]. The present study is focused on improving the thermal conductivity of Emulsion-styrene butadiene rubber (ESBR) which is a cheap alternative to other rubber composites. The disadvantages of ESBR are low thermal conductivity and high heat generation.

Adding fillers with high thermal conductivity to ESBR is proposed as a technique for improving thermal conductivity of ESBR. The purpose of the research is to predict the thermal conductivity of ESBR when filled with fillers of much higher thermal conductivity and also to find out to what extent the filler properties affect the heat transfer capabilities of the composite matrix. The influence of different filler shapes i.e. spherical, cylindrical and platelets on the overall thermal capability of composite matrix is studied, the finite element modelings are conducted using Abaqus. Three-dimensional and two-dimensional models are created in Abaqus to simulate the micro structure of the composite matrix filled with fillers.

Results indicate that the overall thermal conductivity increases with increasing filler loading i.e. for a filler volume fraction of 0.27, the conductivity increased by around 50%. Filler shapes, orientation angle and aspect ratio of the fillers significantly influences the thermal conductivity. Conductivity increases with increasing aspect ratio (length/diameter) of the cylindrical fillers since longer conductive chains are able to form at the same volume percentage as compared to spherical fillers. The composite matrix reaches maximum thermal conductivity when the cylindrical fillers

are oriented in the direction of heat flow.

The heat conductivity predicted by FEM for ESBR is compared with that predicted by mean field theories. At low volume fractions the FEM and mean field theory results are matching. However at high volume fractions the results obtained by the two methods are not in agreement. This is due to the fact that mean field theories do not consider the particle interactions happening at higher volume fractions.

The present analysis can be used to tailor the thermal properties of ESBR for required thermal conductivity for a wide range of applications such as racing tires, electronic gadgets or aeronautical components. In addition, the proposed FEM models can be used to design and optimize the properties of new composite materials providing more insight into the thermal conductivity of composite polymers and aid in understanding heat transfer mechanism of reinforced polymers.

ACKNOWLEDGEMENTS

I would like to sincerely thank my committee members who were more than generous with their expertise and precious time. A special thanks to Dr. Alireza Tabarraei, my advisor, for giving me the opportunity to work with him and for his countless hours of reading, motivating, and most of all patience throughout the entire process. I also take this opportunity to thank Dr. Elliott and Dr. Ogunro for agreeing to serve on my thesis committee.

Finally, I thank all my friends from the University for helping me towards completion of my degree. It has truly been a roller coaster ride with a lot of ups and downs.

DEDICATION

I dedicate my work to my loving parents whose constant support and push for tenacity helped me complete my research.

I also dedicate my work to all my friends, colleagues who not only supported me throughout the process but helped me learn various skills required for my research. A big thanks to my competitors who motivated me to work hard.

TABLE OF CONTENTS

LIST OF FIGURES

LIST OF TABLES

CHAPTER 1: INTRODUCTION AND BACKGROUND

1.1 Introduction

Polymers with high thermal conductivity are becoming increasingly important in wide range of domains ranging from tire treads, electronic packaging, bio-preservation, aeronautics etc and it can lead to high performance and longer service life [2]. Many experimental activities have been performed in the past 10 years to enhance the conductivity of composites. This goal is achieved by reinforcing the low conductivity polymer with fibers of high thermal conductivity. In addition to experiments, finite element modeling (FEM) and theoretical modeling can be used to reduce the product design cycle and to decrease the design and product cost in limited time [3].

In this project we use FEM to study the thermal conductivity of Emulsion-polymerized styrene-butadiene rubber (ESBR) which is made up of two monomers styrene and butadiene and emulsion process is used for polymerization. Due to its remarkable mechanical properties and low manufacturing cost, it is widely used to make the tire tread composites. The main disadvantages associated with ESBR are high heat generation and low conductivity.

In this thesis, we use finite element method to understand the effects of micro fillers on the overall thermal conductivity of ESBR polymer. and finding out effective ways to enhance the thermal properties of the matrix under consideration. Such an understanding will allow us to find effective ways for enhancing the thermal properties of ESBR. The influence of filler properties with various shapes (spherical and prolate), sizes, orientation, volume fraction are studied. The finite element modelings are conducted using Abaqus. Python scripting is used to generate the finite element models. Using python scripting allows us to run multiple iterations and obtain the

ensemble average. Aluminum oxide and carbon nanotubes are considered as fillers in our study. The next section provides a brief introduction on ESBR, aluminum oxide and carbon nanotubes.

1.1.1 Brief introduction to ESBR

Styrene butadiene lies under the class of synthetic rubbers and as the name suggests is made of two monomers styrene and butadiene [5]. Because of very high abrasion resistance and good mechanical properties styrene butadiene rubbers are widely used to make tire tread composites. About 40-50 percent of the tire manufacturers use various types of styrene butadiene rubber (SBR) to make tires treads.

There are mainly two ways by which the process of polymerization takes place, namely emulsion polymerization and solution polymerization. These two methods differ from each other by initiation process and the type of emulsifying agent used. If SBR is processed by emulsion polymerization, ESBR is obtained, on the other hand if SBR is processed using solution technique, SSBR is obtained. The tensile strength, glass transition temperature, and viscosity of ESBR is higher than SSBR and hence the former is widely used.

1.1.2 Brief introduction to carbon nanotubes

Carbon nanotubes are cylindrical tubes that are allotrope's of graphene. They have wide applications in nano technology, optics and material science [7]. It is possible to achieve a very high aspect ratio for carbon nanotubes as compared to other materials and this feature makes them unique. Carbon nanotubes have a very high thermal conductivity, tensile strength, elastic modulus along with good mechanical properties [8]. Carbon tubes are used as fillers in the present study and its various properties are discussed further.

1.1.3 Brief introduction to aluminum oxide

Aluminum oxide is a compound made up of two parts of aluminum and three parts of oxygen. This compound has high thermal properties, good abrasion resistance, high strength and excellent mechanical properties because of which it is widely used in commercial polymer material for high performing applications. The physical properties of Al_2O_3 are described in the next section [9].

1.2 Outline of the thesis

Chapter 2 describes the finite element modeling section to discuss the procedure selecting modeling domains and preprocessing.

The finite element results are presented in chapter 4. In this chapter the effect of various filler properties such as volume fraction, size, orientation for 2D and 3D models are described. This section also describes the results from the analytical methods.

The finite element results are compared with the mean field homogenization equations in chapter 4. The limitations of mean field are also discussed in this study. Finally Chapter 5 concludes the work.

CHAPTER 2: FINITE ELEMENT MODELING

Finite element method (FEM) is a robust method which is widely used to find the solutions of boundary value problems in engineering and mathematics. In any finite element modeling, assumptions are made regarding the physical or geometrical properties of the model under consideration. The present study also stands on some assumptions, these are as follows.

1) Both ESBR (Emulsion styrene butadiene rubber) matrix and filler are isotropic i.e the the thermal conductivity remains constant along one direction in the micro-structure.

2) Over the working temperature range of 328k to 298k, the thermal properties are temperature independent.

3) The temperature is not time dependent therefore at any point of time the temperature profile remains constant in the material.

2.1 Python Scripting in Abaqus

In this Section , the significance of python scripting is discussed and shows a broader aspect of how we can extract the script and modify it according to our needs.

2.1.1 Introduction to scripting

The graphical user interface (GUI) of Abaqus/CAE sends the information to kernel which is the brain of Abaqus/CAE and helps in interpreting the results. It then stores the information to a journal file which is written in python [13].

Abaqus generates several file that store python commands such as replay file, recovery file and journal file. Replay file stores all the information from scratch that the user performs in GUI. Recovery file consists of important information and can be

obtained even if we do not save the model database before exiting. Journal file is one of the main files that contains all the relevant information that the user needs [13].

The journal file contains all the steps that we performed in the GUI in python language. It is then converted to a python file and modified accordingly. Some of the advantages of using a script as follows

1) Ease of running multiple iterations simultaneously and automate repetitive task. The python script can be used to create library of standard materials, mesh size, jobs, boundary conditions etc.

2) Performing a parametric study i.e. a study where some feature of the model is varied and the resulting model is analyzed.

3) Model parameters created in Abaqus can be modified which is used in this study for finding the size of modeling domain or varying filler dimensions and properties.

4) Large bulk of results requested in the history output can be accessed by writing a code in python which reads the output database file and presents the result in a text file.

2.2 Size of the Modeling domain

Modeling domain represents a macroscopic point in the material and is a representative of the micro-structure of the material. It can be seen as analogous to an integration point in finite element method where all the integrals are evaluated numerically depending on the Integration scheme [11].

According to "Drugan" and "Willis" modeling domain is defined as the smallest volume element that statistically represents the matrix composite [12]. It is noted that there exists no fix size for modeling domain and is dependent on the mechanical properties that need to be studied, so the selection of its size becomes a complicated process and hence it becomes important to give a quantitative definition of its size [12].

Determining appropriate modeling domain size is important which captures the

essence of the composite material and the micro structure appropriately. A modeling domain size analysis is performed in which the dimensions of modeling domain are while keeping the aspect ratio and volume percentage constant for each iteration. [20]

The figure 2.1 2.2 shows the results for 2D and 3D modeling domain sensitivity analysis.

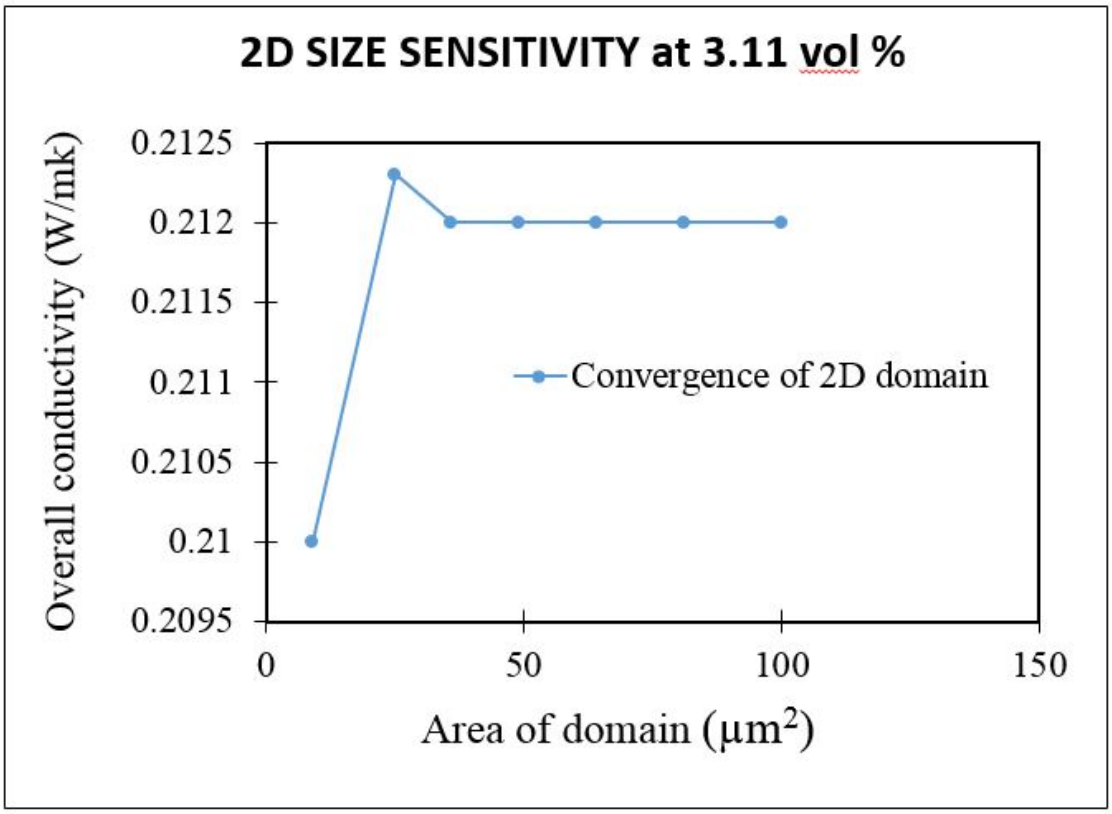

Figure 2.1: Modeling domain Sensitivity 2D

2.3 Modeling

2.3.1 2D Modeling

Two dimensional FEM models are created in Abaqus and is represented by rectangular matrix with spherical and cylindrical fillers dispersed in the matrix region. The two-dimensional matrix regions are modeled using rectangular geometry of side length of 10 µm. The smallest radius of spherical filler inclusion used in the study has a dimension of 0.1 µm. The carbon-nanotubes (cylindrical fillers) has the smallest aspect

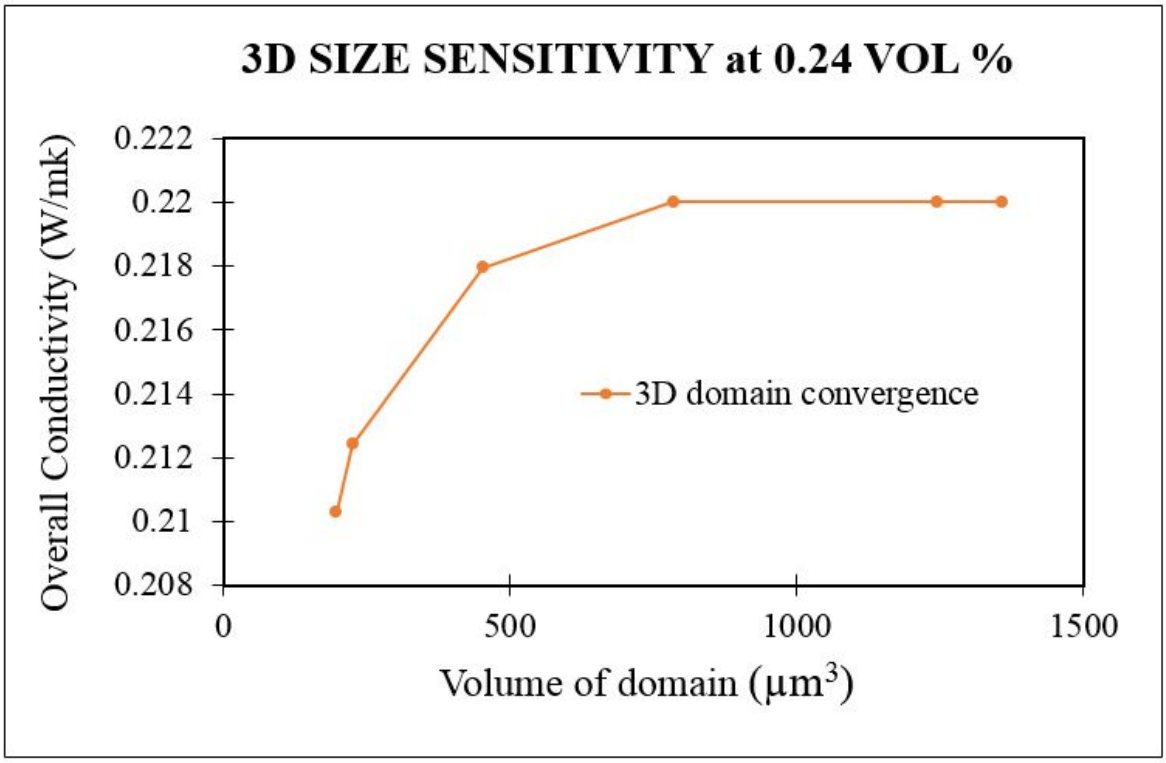

Figure 2.2: Modeling domain Sensitivity 3D

ratio of 10 µm and varies up to 60 µm for various simulations. Fillers are randomly dispersed in the matrix region of ESBR and the respective region of ESBR where the filler is dispersed, is removed. 'Partition' method is used in abaqus to carry out this process. Python scripting is used to randomly generate the spherical and cylindrical fillers in the matrix. Figure 2.3 shows spherical fillers in matrix and Figure 2.4 shows randomly dispersed rectangular fillers.

2.3.2 3D Modeling

The three dimensional FEM model consists of a cylindrical matrix region with spherical and cylindrical fillers randomly dispersed in the matrix. The cylindrical modeling domain is modeled in Abaqus having a fixed radius = 5 µm and fixed height = 15 µm. Python scripting is used to randomly disperse the spherical and cylindrical fillers in the matrix region. The spherical filers for 3D modeling domain has a minimum radius = 0.1 µm and the aspect ratio varies between 10 to 60. Figure 2.5 and

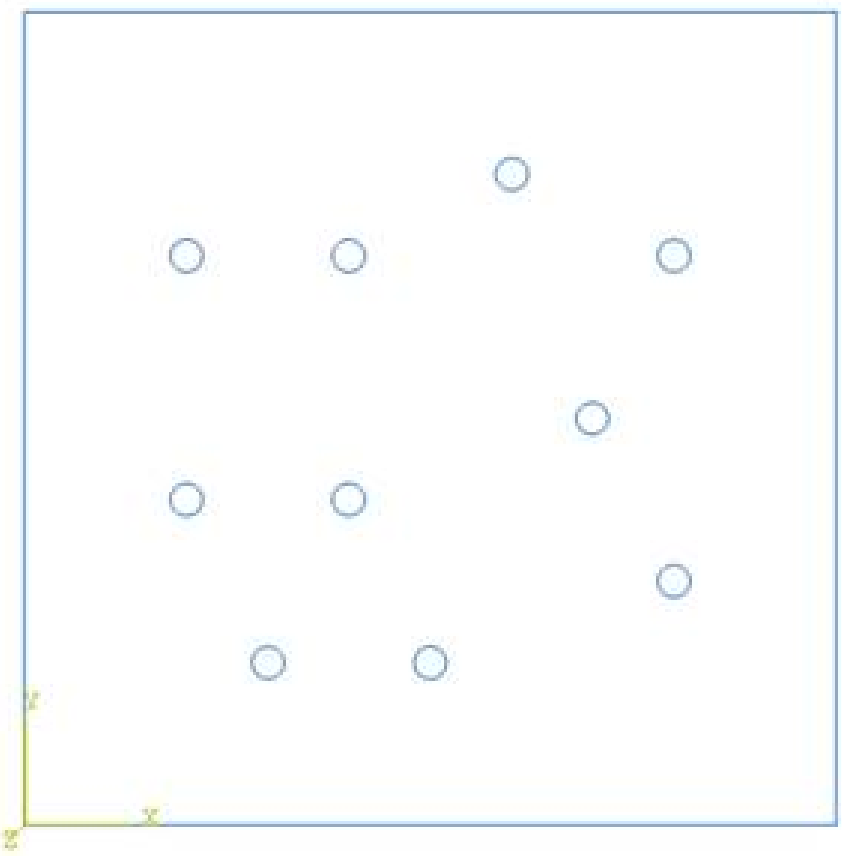

Figure 2.3: 2D FEM model of ESBR and SPF

2.6 shows the 3D modeling domain with spherical and cylindrical fillers.

In the present study modeling domain size analysis is performed, the Volume of domain chosen for this study varied from 400 to 1500 cubic micrometers and the effect of this parameter on overall conductivity is observed. Modeling domain's of various sizes are tested at the same volume fraction till the convergence or stability is achieved.

The trend initially increases as the size of the domain is increased and after reaching a stable size the conductivity becomes stable. The various sizes chosen for the study has same aspect ratio, so the length and diameter of the modeling cylindrical domain is varied such that the ratio of length/diameter remains same.

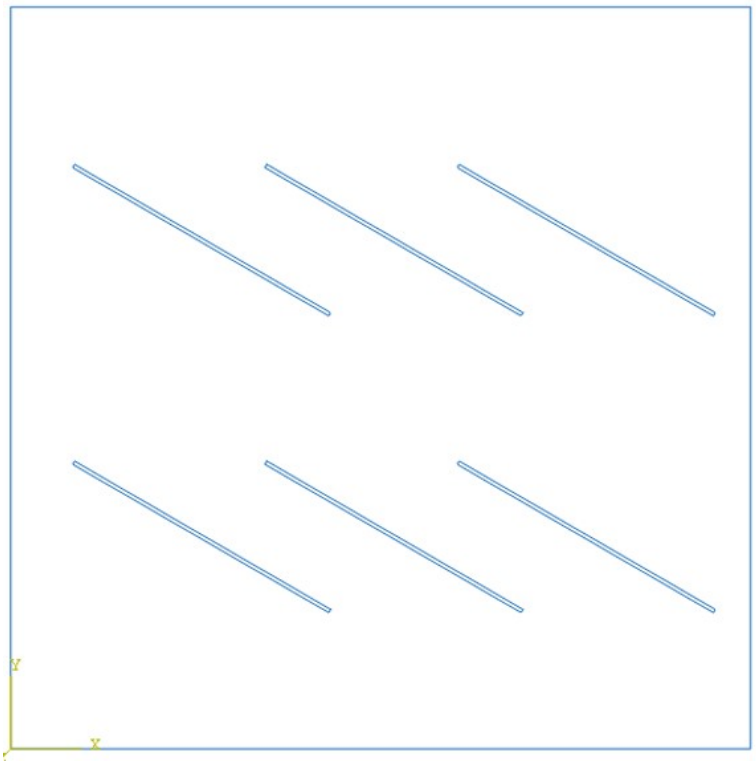

Figure 2.4: 2D FEM model of ESBR and CNT

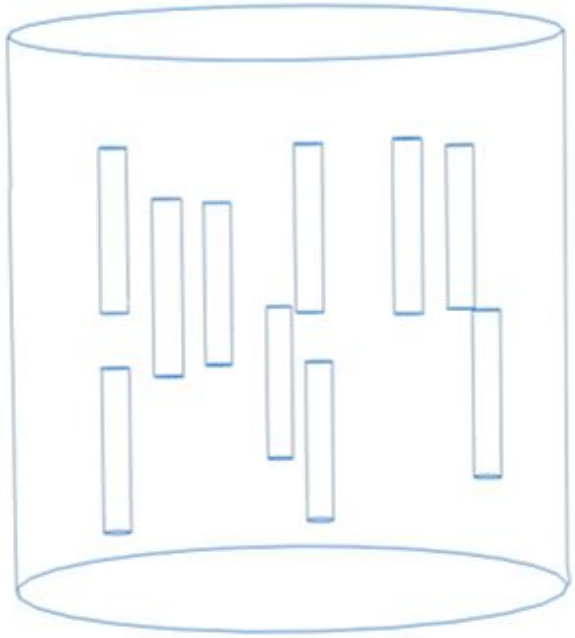

Figure 2.5: 3D FEM model of ESBR and CNT

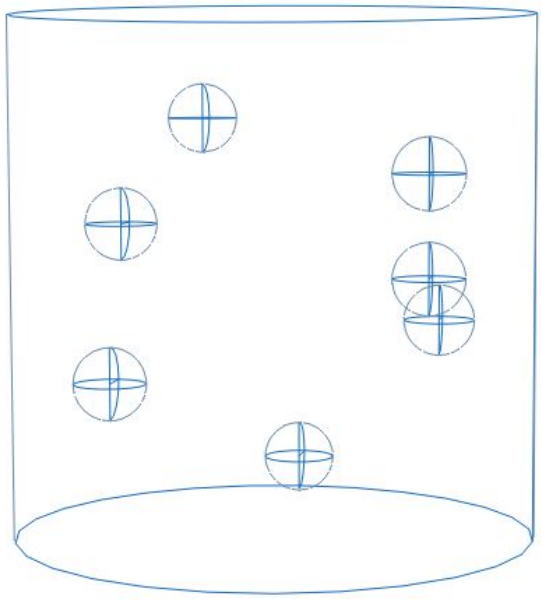

Figure 2.6: 3D FEM model of ESBR and SPF

The micro-structure of the 2D and 3D models changes depending on different filler properties such as aspect ratio, size, shape, volume fraction of filers and other properties discussed further ahead in the section. At least 25 iterations are performed for different dispersion patterns and the results are averaged to obtain a stable predicted value of thermal conductivity.

2.4 Material Properties

Physical properties are the properties that can be measured without changing the chemical identity of the material. Once the modeling domain is modeled in Abaqus, it is very important to assign correct physical properties to the finite element model. Assigning exact physical properties ensure that the result obtained is credible.

The physical properties of ESBR and conductive fillers are provided in the Table 2.1. Al_2O_3 fillers are both spherical and fibers, the CNT are modeled in the form of hollow cylindrical fillers.

Table 2.1: Physical properties of ESBR and conductive fillers

Physical properties			
Material	Density ($\frac{g}{cm^3}$)	Particle shape	Thermal conductivity($\frac{W}{mk}$)
Matrix ESBR	0.93	-	0.2
Al_2O_3 Filler	3.95	Spherical	10.0
CNT	1.30	Tubulous	120

2.5 Boundary conditions

2.5.1 Steady State heat conduction

Steady state heat conduction refers to the transfer of heat energy from high temperature particle to lower energy particles. Since its a steady state all derivatives of temperature with respect to time are zero and all other partial derivatives of temperature with respect to space may have a non zero value [14]. For a steady state heat conduction, we require that,

$$q_{in} = q_{out} = 0 \tag{2.1}$$

where, q_{in} is the heat flow in and q_{out} is the heat flow out

The heat conduction is directly proportional to the temperature difference and surface area but varies inversely with the thickness. It can be written as,

$$q_{cond} = -kA\frac{dt}{dx} \tag{2.2}$$

where, q is the heat flux density in 'W/m^2'
k is the thermal conductivity in 'W/mk'
A is the surface area in'm'
and dt/dx is the temperature gradient or slope of the temperature curve in 'K/m'

Boundary conditions are the type of external conditions that needs to be prescribed on the geometry under consideration.

For the present study, one directional heat transfer problem, constant temperature is applied at the top (328 k) and bottom (298 k) surfaces of the modeling domain. The side surfaces are kept adiabatic which means it has zero heat flux. Isothermal boundary conditions are applied at the top and bottom surfaces and adiabatic on the sides parallel to the direction of heat flux. The 2D and 3D boundary conditions are shown in the figure 2.7 and figure 2.8.

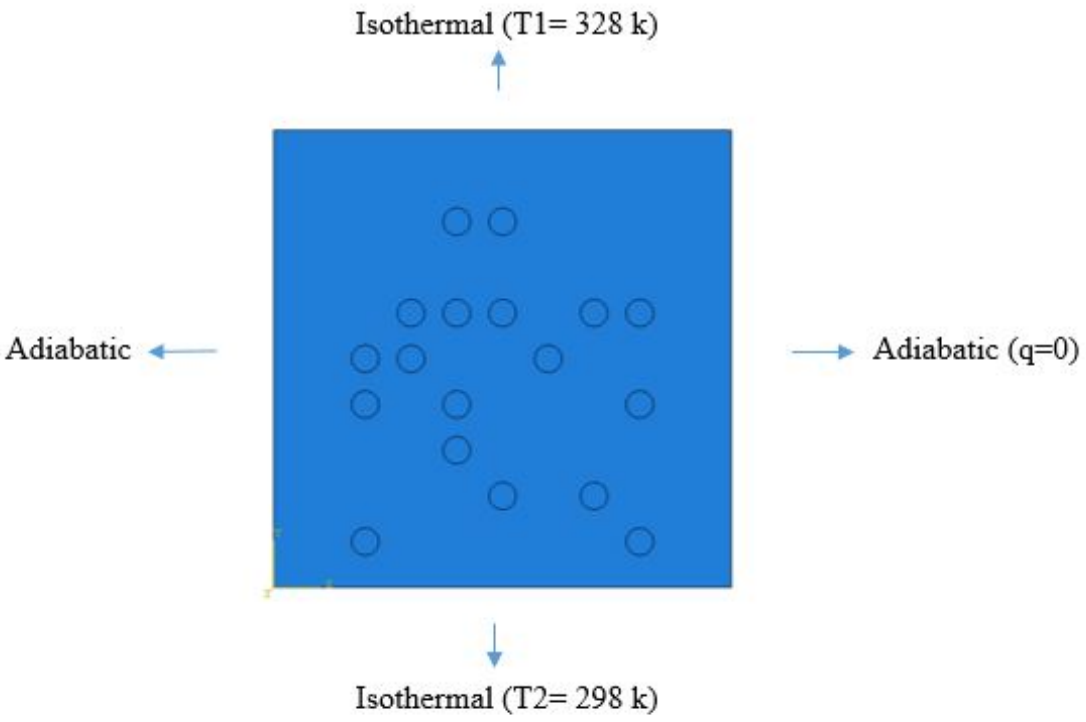

Figure 2.7: Overall conductivity vs parts per hundred resin for 2D SPF

For adiabatic surfaces,

$$q = -k\frac{dt}{dx} = 0 \tag{2.3}$$

For top isothermal surfaces of ESBR composites,

$$T = T_o = 328k \tag{2.4}$$

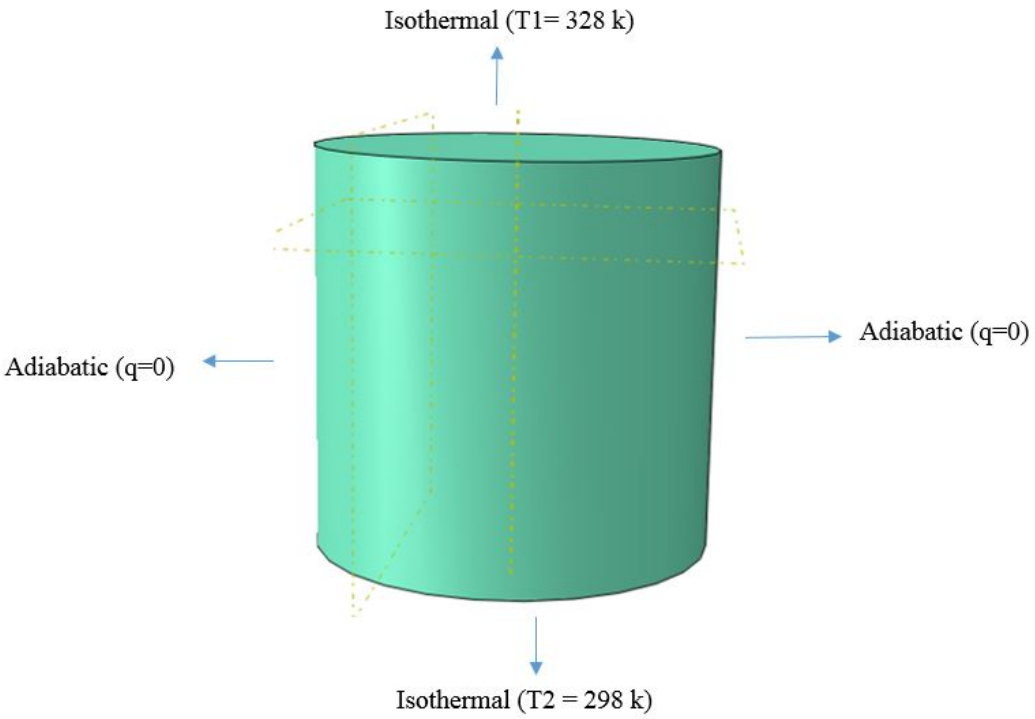

Figure 2.8: Overall conductivity vs parts per hundred resin for 3D SPF

For bottom isothermal surfaces of ESBR composites,

$$T = T_1 = 298k \tag{2.5}$$

Two different sets are created for both 2D and 3D models. The sets contain the temperature data of all the nodes where the temperature boundary condition is prescribed. The heat flux is calculated by averaging the heat flux from all the nodes across the top and bottom surfaces of the modeling domain.

2.6 Meshing

Meshing is a very important part of pre-processing as it determines the model's solution time, precision and quality [1]. Mesh sensitivity analysis is performed to accurately determine the mesh size for the spherical particle filler and the carbon-nano tubes. Figure 2.9 and figure 2.10 shows the converged results with heat flux as

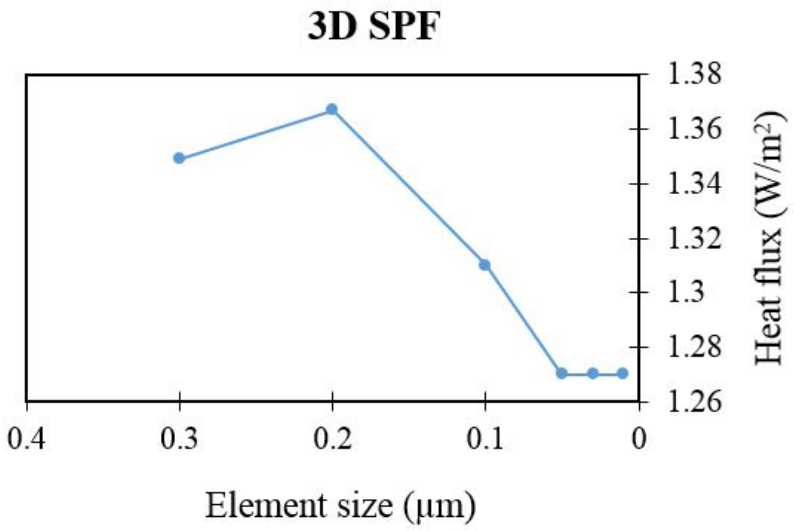

Figure 2.9: Mesh convergence plot for 3D SPF

the independent parameter and mesh size as the dependent parameter.

The results starts to converge at 0.5 µm, so it is taken as the seed size for 3D spherical Particle filler and 0.1 µm for carbon-nano tubes. Taking these seed sizes the model is meshed using a DC2D4 - 4 node linear heat transfer quadrilateral element for 2D modeling domain and DC3D10-10 node quadratic heat transfer tetrahedron element for 3D modeling domain.

Figures 2.11, 2.12, 2.13, 2.14, 2.15, 2.15, 2.17, 2.16 shows the meshed models of 2D and 3D for spherical particle filler and carbon nanotubes.

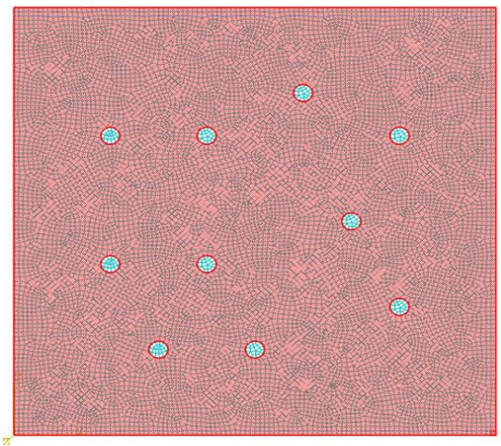

Figure 2.11: 2D meshed spherical fillers

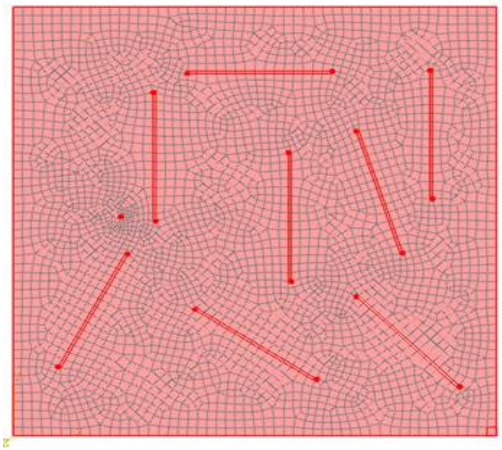

Figure 2.12: 2D meshed rectangular fillers

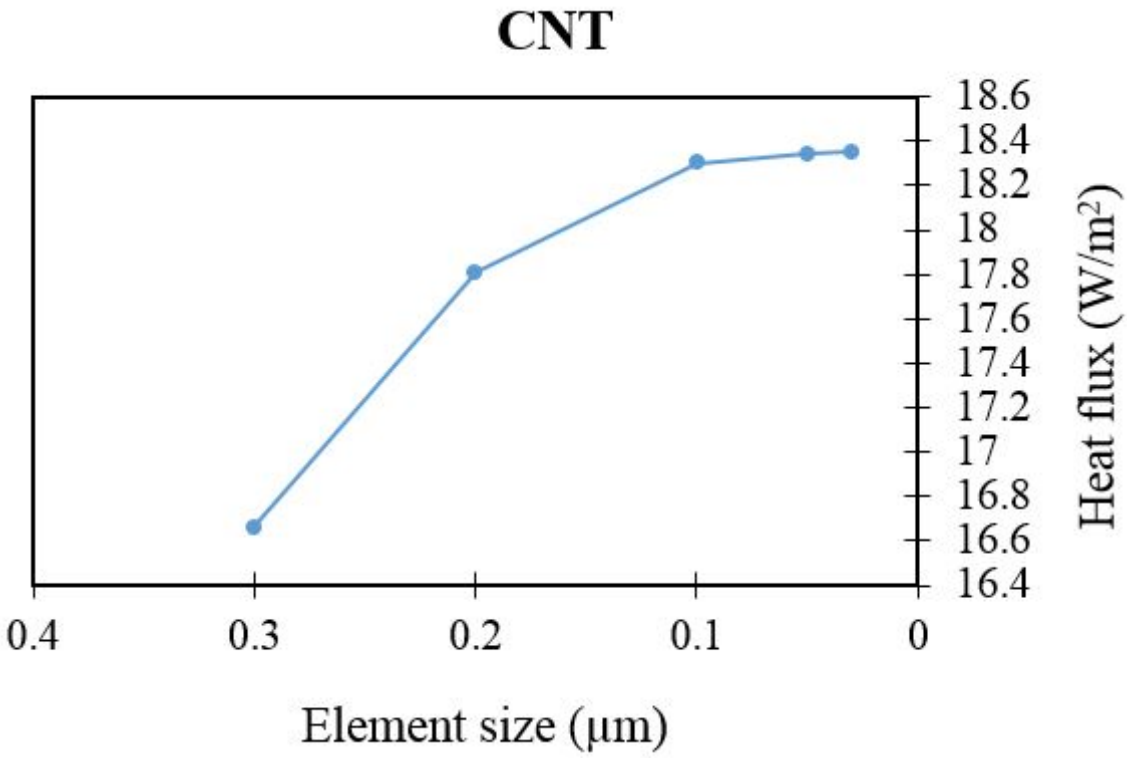

Figure 2.10: Mesh convergence plot for 3D CNT

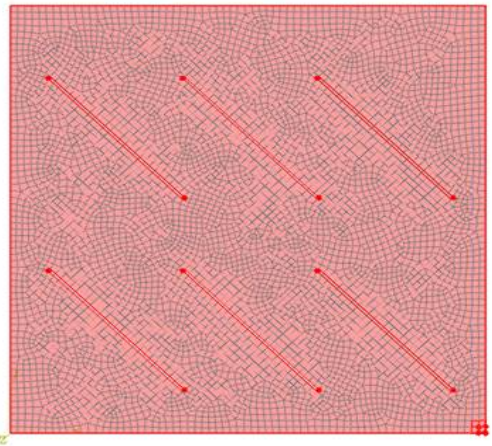

Figure 2.13: 2D meshed rectangular incline fillers

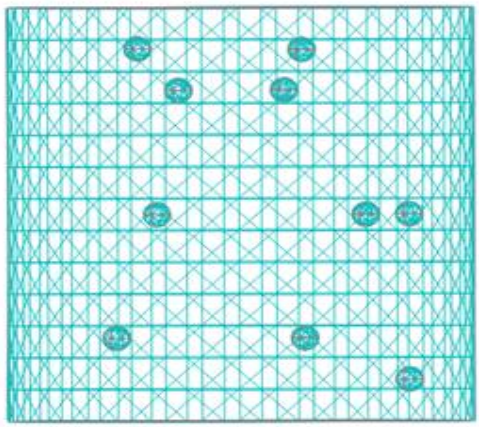

Figure 2.14: 3D SPF meshed

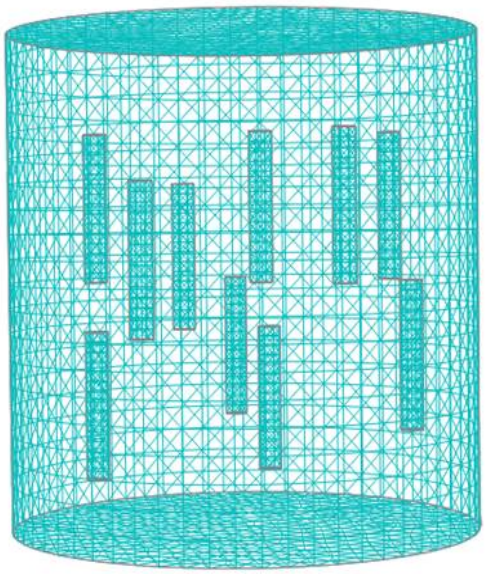

Figure 2.15: 3D meshed CNT's in one-direction

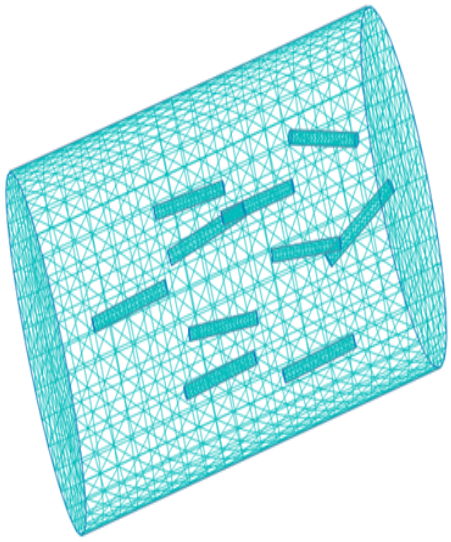

Figure 2.16: 3D meshed random CNT's

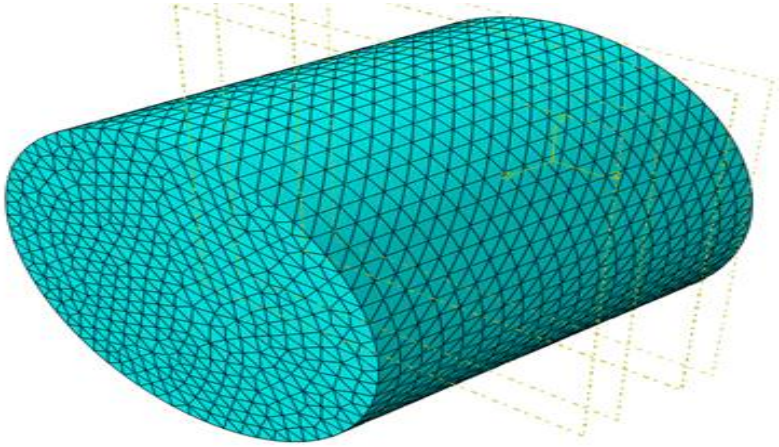

Figure 2.17: 3D meshed modeling domain

2.7 Post-processing

After the model is meshed [1], assigned physical properties, applied boundary conditions, the job module is used for creating the job and run the analysis. This stage is called solving where the software performs numerical integration and computes the results wherever requested.

Since there is a large volume of data that needs to be processed graphical visualiza-

tion is important. But, as there are a large number of output database files, a python script is written which reads the result from all the jobs and writes it to a text file which reduces the task of opening the GUI for such a large number of simulations. The nodal temperature plots and heat flux plots for various 2D and 3D modeling domain models are shown in the following figures 2.18, 2.20, 2.19, 2.22, 2.21

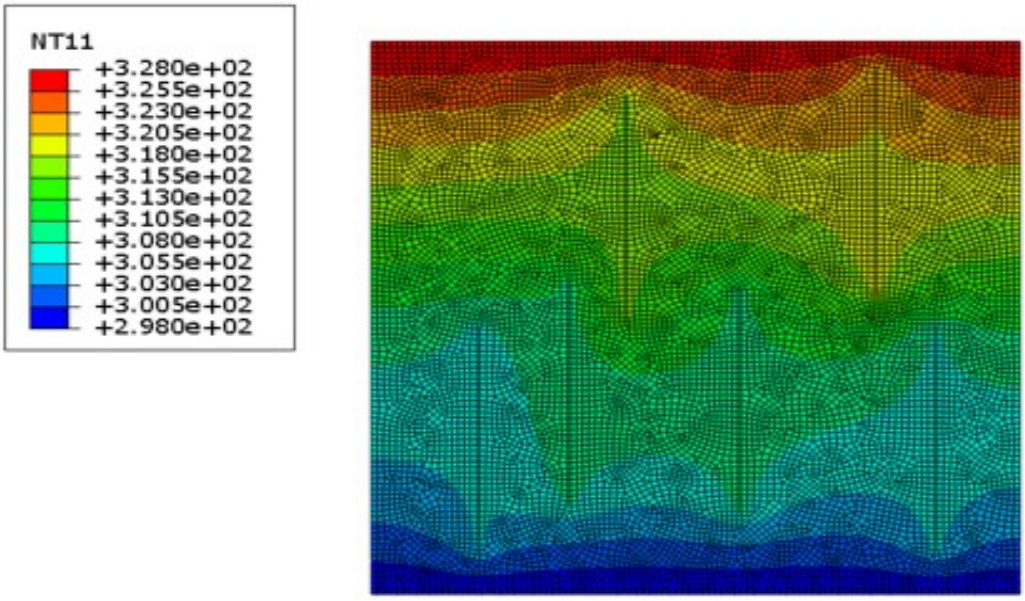

Figure 2.18: 2D CNT Nodal Temperature plot

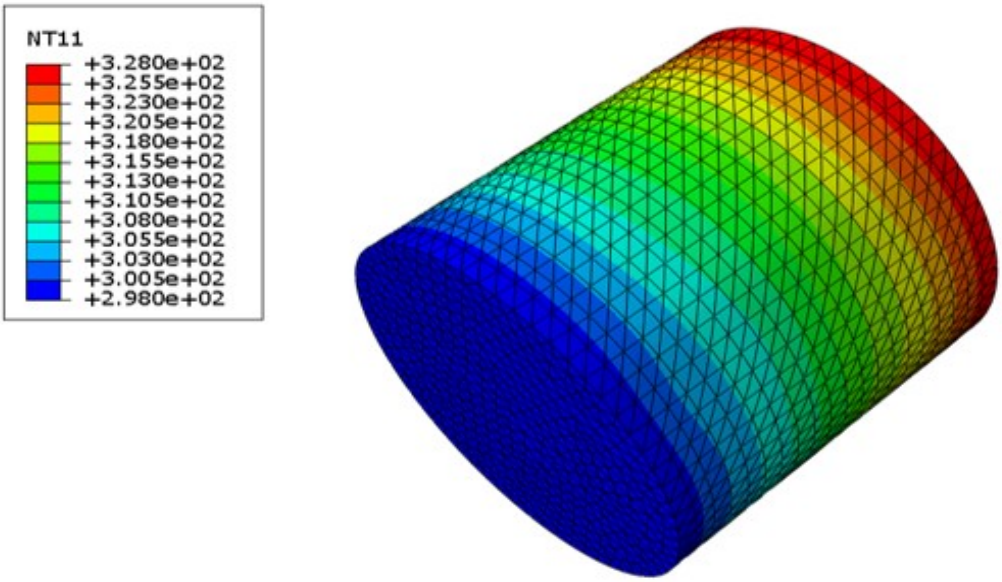

Figure 2.19: 3D Nodal Temperature modeling domain

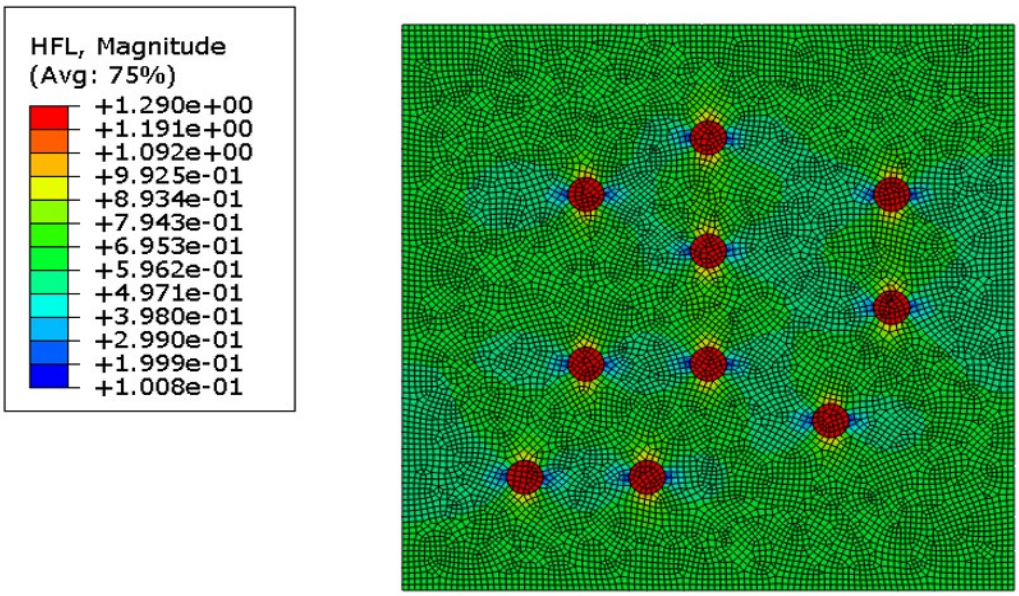

Figure 2.20: 2D SPF HFL plot

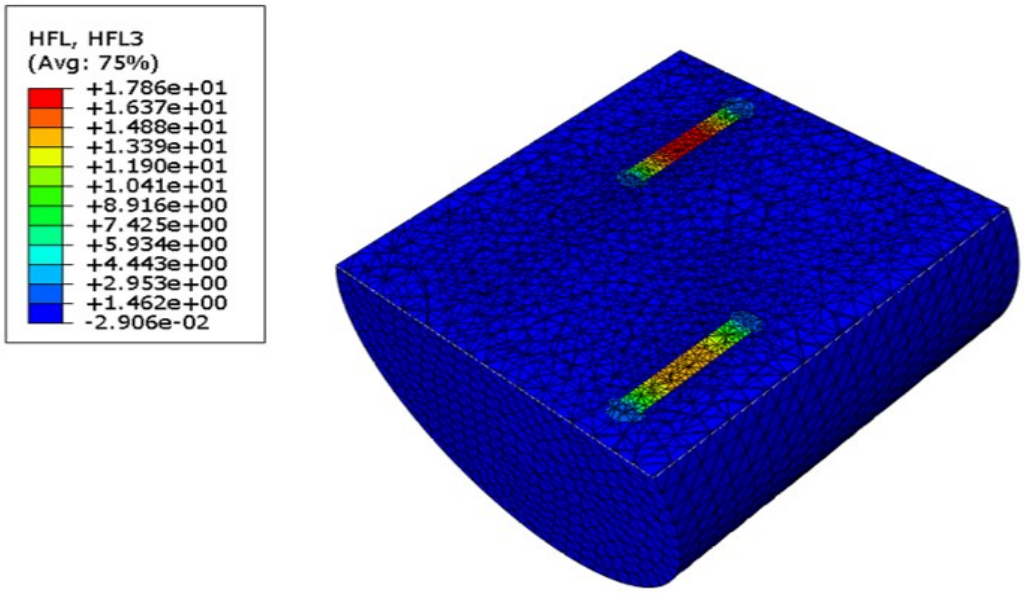

Figure 2.21: 3D Heat flux plot

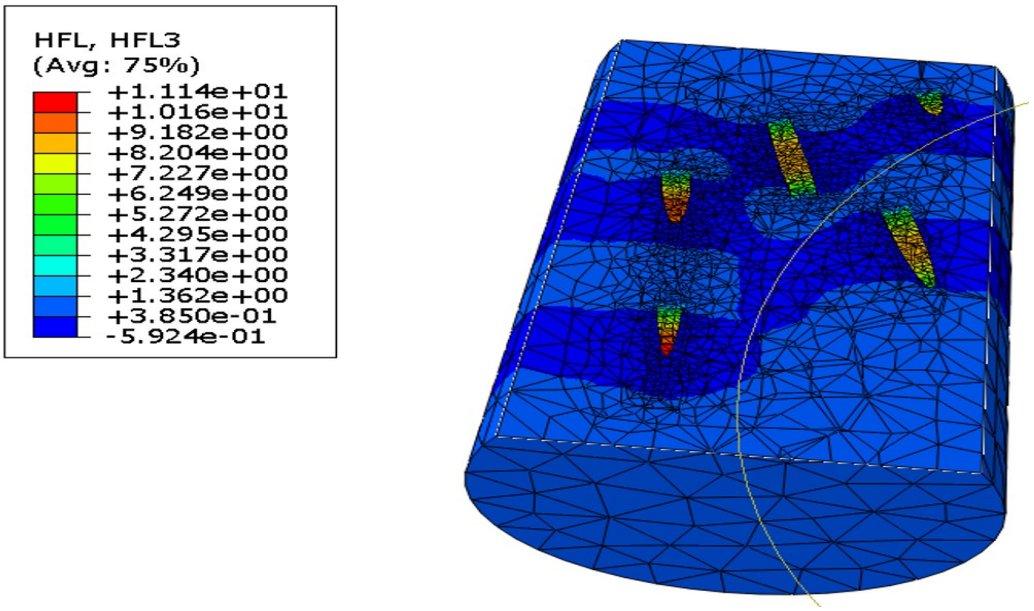

Figure 2.22: 3D HFL random CNT

CHAPTER 3: RESULTS

3.1 Parametric studies

3.1.1 Effect of increasing volume percentage on the overall conductivity

The table 3.1 3.2 shows the data for phr and conductivity for 2D fibers of aluminium oxide and 3D spherical particle fillers of aluminium oxide. The figure 3.2, 3.3 shows the plot of overall thermal conductivity versus the volume percentage of the inclusions in the matrix. The volume percentages of 3.2%, 6.2%, 7.9%, 14.36%, 18.8%, 21%, and 25% are chosen for the present study and overall conductivity is calculated.

Table 3.1: Data for volume percentage/parts per hundred resin and overall conductivity (2D SPF)

Vol% / phr	Overall Conductivity(W/mk)
3.2% / 13	0.2124
6.2 % / 26	0.2280
7.9 % / 33	0.233
14.36%/ 53	0.271
18.84% / 80	0.29
21 % / 93	0.326
25 % / 105	0.345

Table 3.2: Data for volume percentage/parts per hundred resin and overall conductivity (3D SPF)

Vol% / phr	Overall Conductivity(W/mk)
3.2% / 13	0.217
4.4 % / 26	0.224
9.09 % / 33	0.248
12.47%/ 53	0.264
16.82% / 80	0.287
23.7 % / 100	0.319

It is seen that the thermal conductivity is varying linearly with the increasing volume percentage or parts per hundred resin for both 2D and 3D models. 2D models agreed well with the experimental data from the research paper "Thermal conductivity of micro/nano fillers [1] at higher filler loadings while 3D models agreed well at lower filler loadings. This is because at lower filler loadings, not many particles are able to form conductive chains, so the high conductive fillers contribution seemed to be less then matrix which resulted in lower overall thermal conductivity. But once the high conductivity fillers reaches its percolation threshold, the overall conductivity starts increasing with slight increase in volume percentage. This can be explained by the following concept of percolation model.

When the amount or volume fraction of filler in an modeling domain is increased beyond a certain point, the fillers start interacting with each other. As the fillers have high thermal conductivity than the matrix present in the modeling domain, heat transfer chains are formed through which the heat is easily transferred due to high conductivity filler-filler interaction. When such conductivity chains are formed,

it causes a significant increase in the thermal conductivity of composite. The following figure shows the phenomenon of percolation modeling [10].

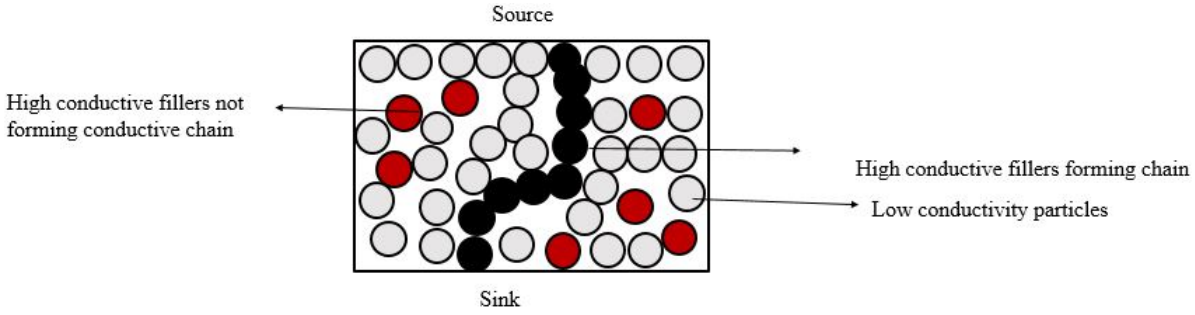

Figure 3.1: Heat transfer enhancement, in particulate composite

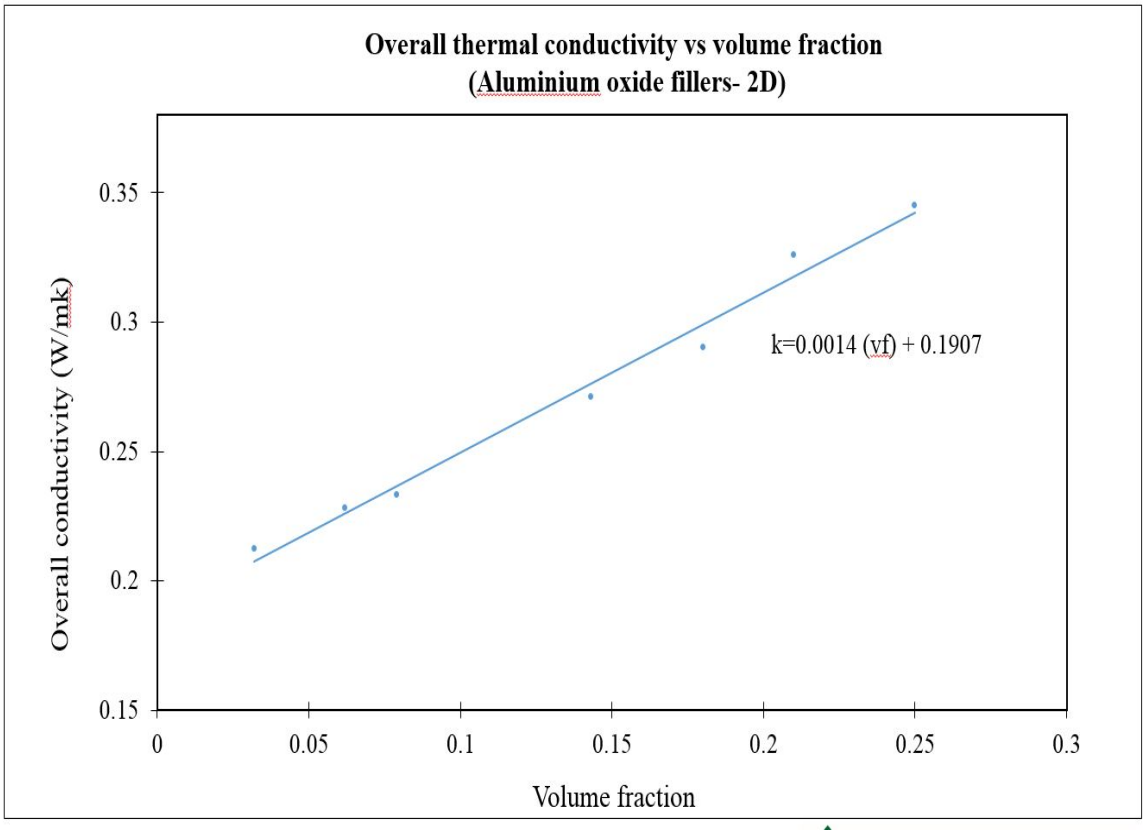

Figure 3.2: Overall conductivity vs volume fraction for 2D SPF

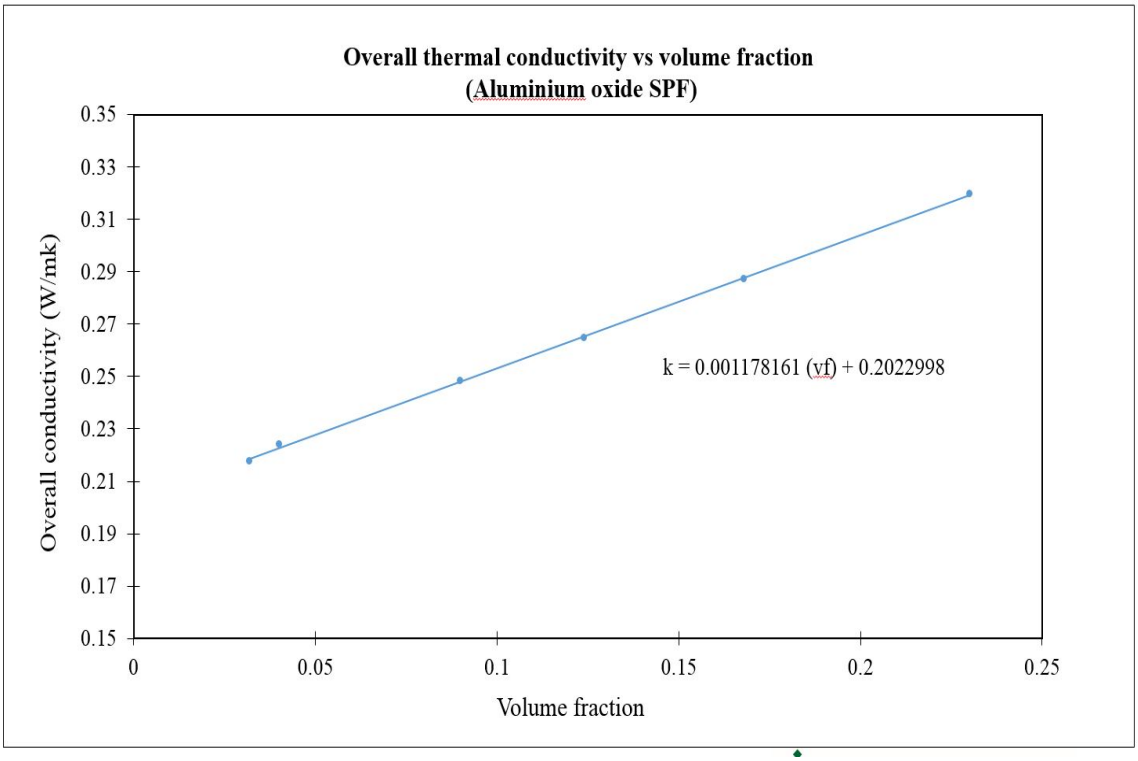

Figure 3.3: 3D FEM model of ESBR and SPF

3.1.2 Varying number of inclusions at constant volume fraction

Study is performed to see, how the number and size of inclusions contribute to enhance the overall effective thermal conductivity. We studied 5 different cases of 3.2%, 8.10%, 14.3%, 18% and 27% volume fractions. In this study the number and diameter of the inclusions are varied keeping the volume percentage constant. Volume percentages of 3.2%, 8.10%, 14.3%, 18% and 27% are chosen for the analysis. When the number of inclusions are increased, the diameter of those inclusions are decreased accordingly to keep the volume percentage constant. So the inclusions will have larger diameter when their numbers are less and vice versa.

The overall thermal conductivity (W/mk) versus the number of inclusion plot is shown in figure 3.4.

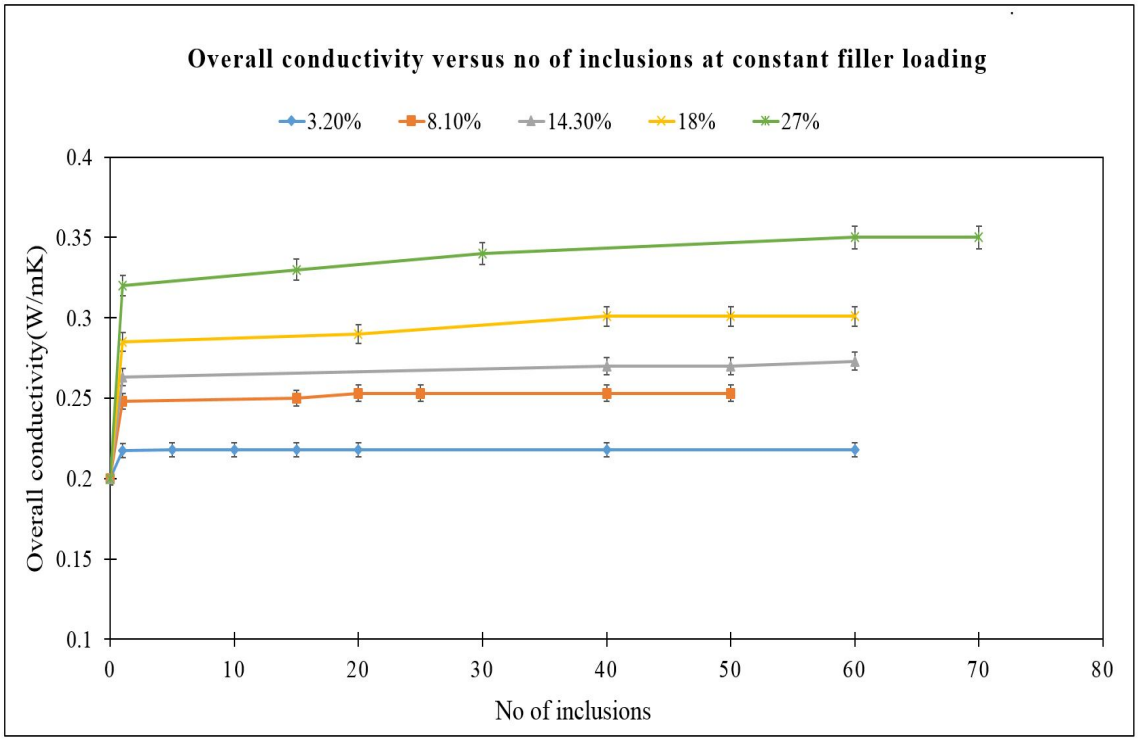

Figure 3.4: Overall conductivity vs no of inclusion

We see that at lower filler volume fraction of of 3.2%, 8.10% and 14.3%, the graph remains horizontal, as there is no significant increase of overall thermal conductivity but at higher filler loadings of 18%, 27%, the conductivity increases after certain number of inclusions. This is because at lower filler loadings the fillers are not able to touch each other and it doesn't reach its percolation threshold because of which there is no formation of conductive chains and the matrix shows lower thermal conductivity. However at higher volume percentages, the fillers are able to form conductive chains even at lower number of inclusions because the size of inclusion at higher volume percentages will be more than the corresponding size at lower volume fraction. To explain this phenomenon, for example: at 60 inclusions, the radius of inclusion at 3.2% is 0.46 µm whereas at 27% and with the same number of inclusion, the radius is 0.86 µm.

3.1.3 Analysis of variance test

An analysis of variance (ANOVA) test is performed to prove the significance of the results at higher filler volume percentages. The one way ANOVA compares the mean between groups to determine if they are statistically significant from each other.

ANOVA test is performed for filler volume fraction of 18% and 27%. The results shows that the F-ratio, which is the measure of systematic variation to unsystematic variation is much greater than 1, which indicates that the results are significantly different, when the number of inclusion is 1 and when the number of inclusions are 60 for the two cases of volume percentages of 18% and 27%.

This analysis clearly highlights the importance of size effect and shows that the size of inclusions plays a significant role in improving the thermal conductivity of fillers for higher volume fraction polymer matrix composite models.

3.1.4 Effect of Aspect ratio of CNT's on overall conductivity

Aspect ratio for a CNT is defined as the ratio of its length to diameter (L/D). Analysis has been performed for 3D CNT's to see how the aspect ratio influences the overall conductivity of matrix with increasing volume percentage. In this analysis the diameter of the cylindrical tubes is kept constant and the length is varied to get cylindrical tubes with different aspect ratios. Python script is modified to get at least 20 different dispersion patterns for the cylindrical fillers oriented in the direction of heat flux at different volume percentages for each aspect ratio and ensemble averaging is done for the respective volume percentage to get a stable predicted value of thermal conductivity. The study was performed for volume percentages of 0.3%, 0.65%, 1%, 1.7% and 2.3%.

The figure 3.5 shows the plot of overall conductivity vs volume percentage at an aspect ratio of 30 and 60 respectively.

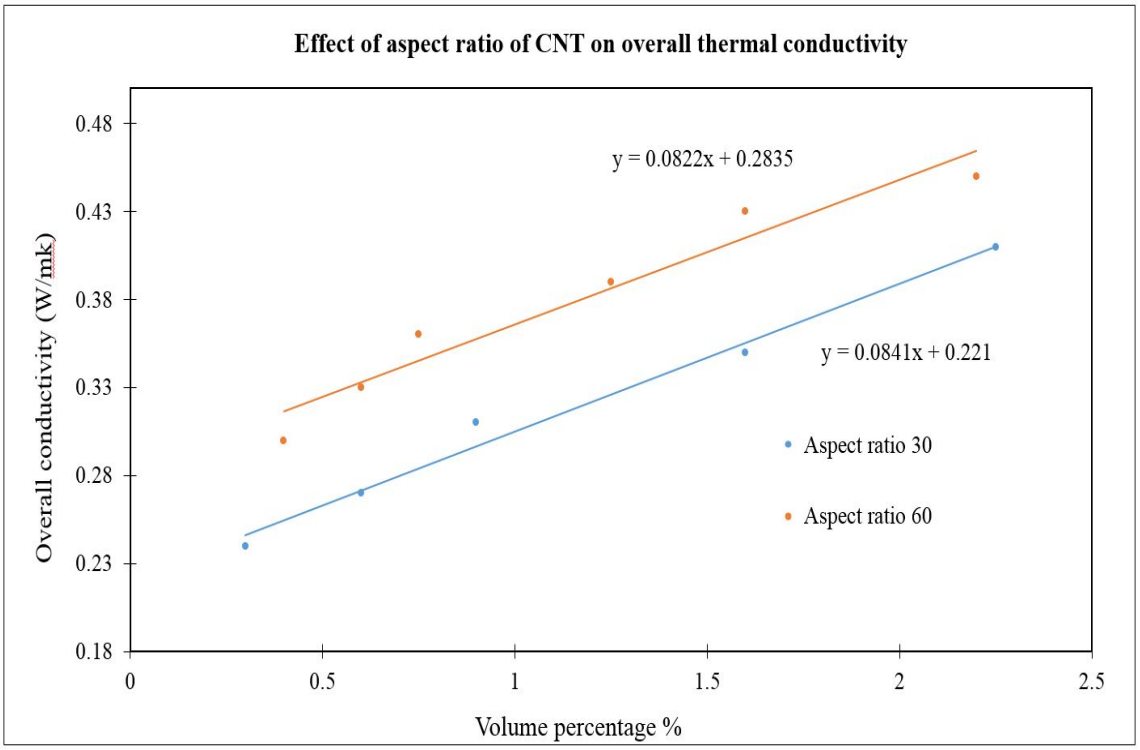

Figure 3.5: Overall conductivity vs volume percentage for different aspect ratio

The results shows that for a particular aspect ratio, the overall conductivity is increasing, it also highlights that for two different aspect ratios and at the same volume percentage, the overall conductivity is significantly increasing. For example: at constant volume percentage of 0.56, the overall increase in conductivity is around 22% for two different aspect ratios. This may be because that now even at low filler volume percentage conductive chains are easy to form because the length is more at higher aspect ratios.

Hence, the results from this shows that aspect ratio is a significant factor in determining the overall thermal conductivity of fillers.

3.1.5 Effect of orientation of fillers for 2D platelets

The effect of orientation angle of platelets are expected to have a major effect on the overall conductivity of matrix or composite. Therefore, it is very important to study this effect to deepen our understanding of the thermal conductivity.

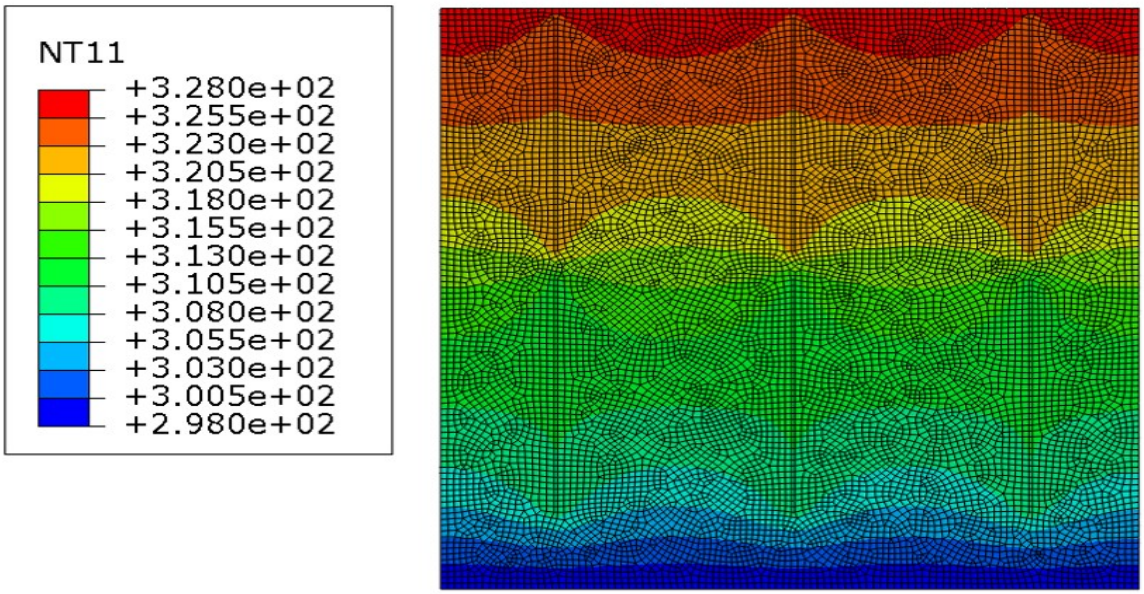

Figure 3.6: Nodal temperature plot when the fillers are oriented in the direction of heat flux

The Figure 3.8,3.9,3.10,3.11,3.12,3.13 and 3.14 shows the heat flus plots of 2d platelets fillers oriented at various angles of 0 °, 15 °,45 °, 90 °. The 0 ° platelets refers to the platelets oriented in the direction of heat flux and 90 ° refers to the platelets oriented perpendicular to the direction of heat flux.

Figure 3.6 and Figure 3.7 shows the nodal plots for plates rotated in the direction of heat flux and randomly oriented. When the fillers are oriented in the direction of heat flux they are able to distribute the temperature much more effective, however when the fillers are oriented perpendicular to the direction of heat flux there is no redistribution of temperature from higher gradient to lower gradient.

The heat flux plots show that as the platelets's orientation changes from 0 ° to 90 °, the heat flux reduces, indicating that the heat transfer capability of the domain matrix is now reduced. This is due to the fact that longer conductive chains are formed when the filler is oriented away from the direction of heat flux. The results show that orientation angle is a very important factor in tuning the thermal conductivity. In comparison to that, the volume percentage of platelets is a minor factor.

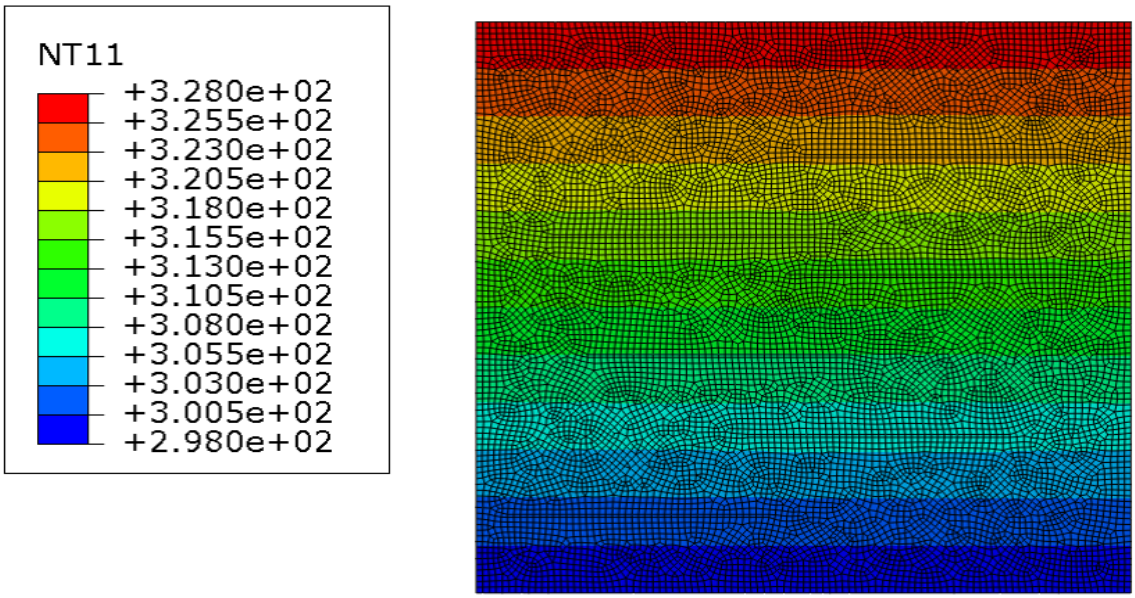

Figure 3.7: Nodal temperature plot when the fillers are oriented perpendicular to the direction of heat flux

3.2 Effect of varying conductivity of spherical particle fillers

In order to gain more insight for designing the thermal conductivity of fillers and ESBR composite and also to find a way to tailor the properties of filler. Three dimensional finite element models are created by modifying the python script in which the conductivity of fillers are varied from 0.01 to 12 times the thermal conductivity of filler (i.e 10 W/mk). The conductivity is varied from 0.1 W/mk to 120 W/mk.

Table 3.3: Varying the orientation angle of the inclusions at constant volume percentage of 1.2% at an aspect ratio of 80

Orientation angle (degrees)	heat flux (W/m^2)	Overall conductivity(W/mk)
0°	-1.131	0.396
15°	-1.132	0.377
30°	-0.97	0.323
45°	-0.831	0.277
60°	-0.704	0.234
75°	-0.634	0.211
90°	-0.6075	0.202

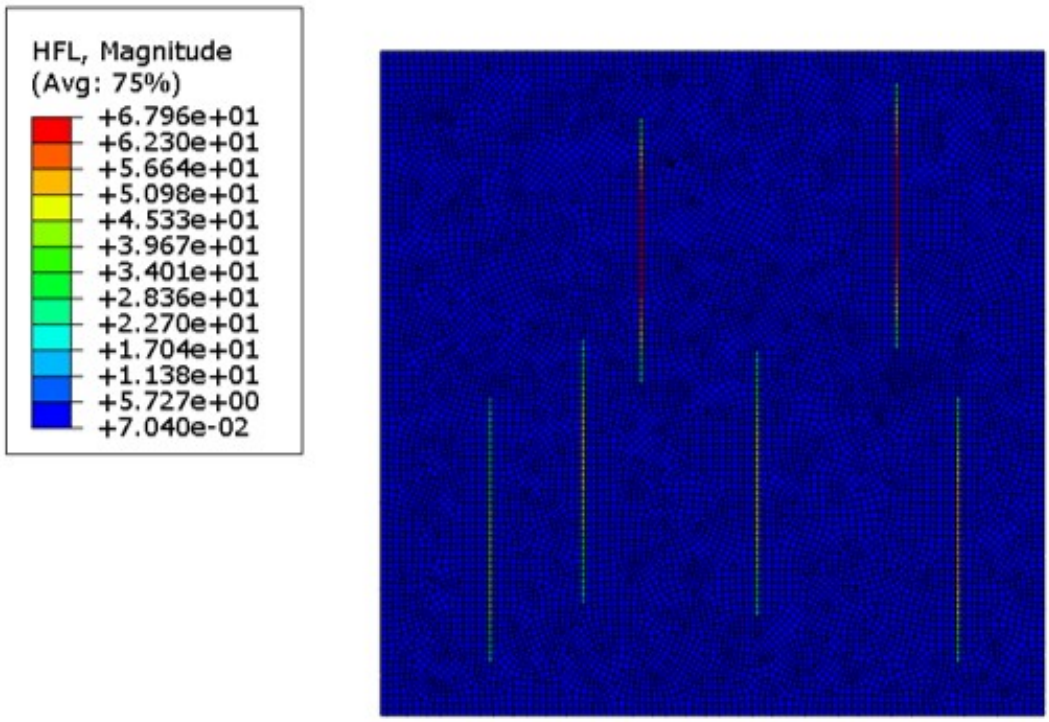

Figure 3.8: Heat flux plot for 2D platelets oriented at 0 °

The simulations are performed for three different volume fractions at 5 %, 14% and 20%. The figure 3.16 shows the plot of overall thermal conductivity vs the increasing conductivity of filler for these three volume fractions.

It is seen from the results that a plateau is reached for all the volume fractions when the filler conductivity is beyond a certain value. For 5% volume fraction, the plateau is reached at around 10 W/mk, for 14% , the plateau is reached around 10 W/mk and at around 25 W/mk for 20% volume fraction.

Therefore, we see that it is imprudent to use higher thermal conductivity fillers of more that 30 W/mk when the volume fraction is less that 0.25 as it will have no significant effect on the overall thermal conductivity of ESBR composite. The reason for this is may be because that the matrix has reached its percolation limit and no more conductive chains are able to form at the same volume percentage. One theory also tells us that when the volume percentage of fillers is much more than 60% , then increasing the thermal conductivity of filler makes more sense, as now they might be

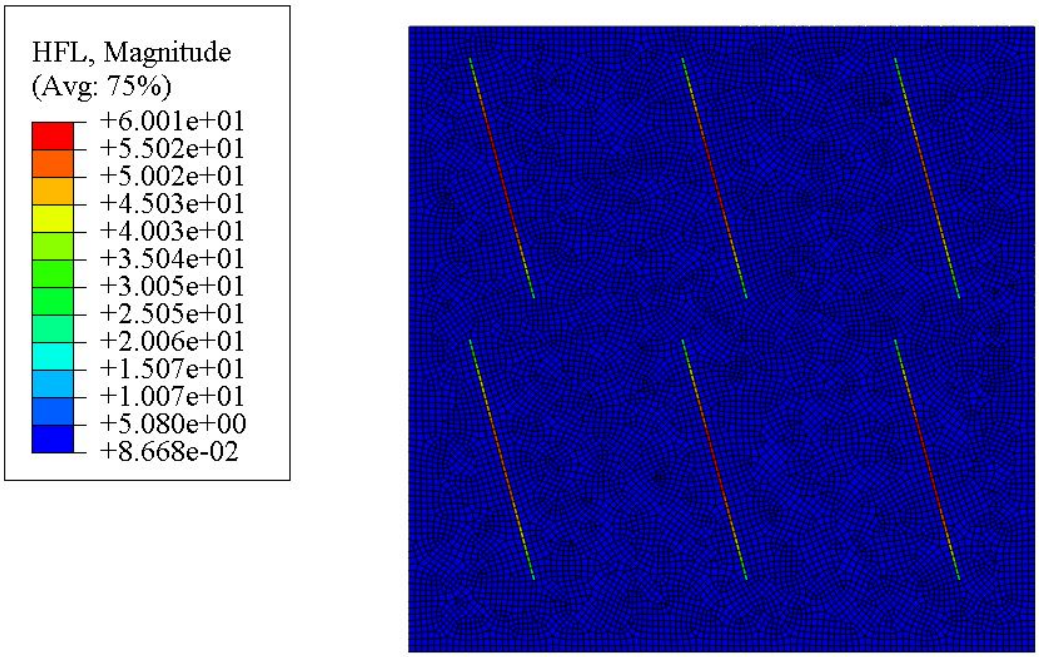

Figure 3.9: Heat flux plot for 2D platelets oriented at 15 °

able to form conductive chains via agglomeration.

3.3 Effect of varying conductivity of carbon nanotubes

The intrinsic conductivity of cylindrically shaped fillers are varied from 10 W/mk to 400 W/mk to see the effect of filler conductivity on the overall conductivity of the matrix. Analysis is performed on three volume percentages of 0.44, 1 and 1.2 to observe the effect of filler conductivity on different concentration ratios. The figure 3.17 shows the plot of overall thermal conductivity versus the varying filler conductivity.

The results show that a percolation limit is reached for all the volume fractions at a certain conductivity of fillers depending on the volume percentage. The results indicate that increasing or designing the conductivity of fillers beyond 150 W/mk is of no use when the filler volume fraction is less than 1.2 % as no more conductive chains are formed beyond this range. The sensitivity analysis sets an upper limit for designing fillers of spherical shape and carbon nanotubes.

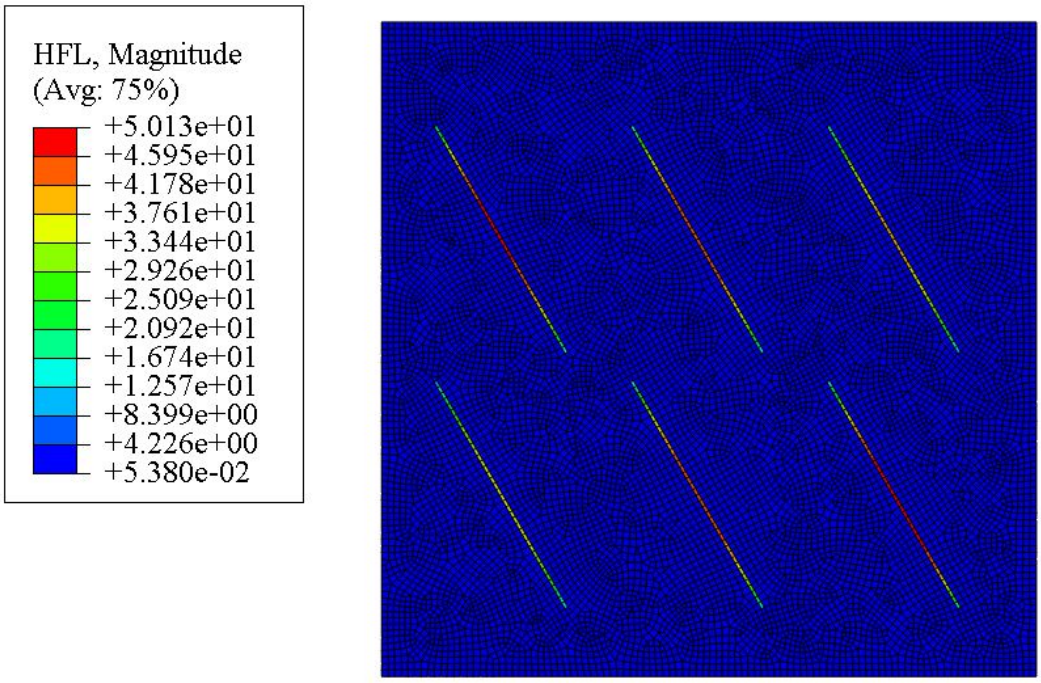

Figure 3.10: Heat flux plot for 2D platelets oriented at 30 °

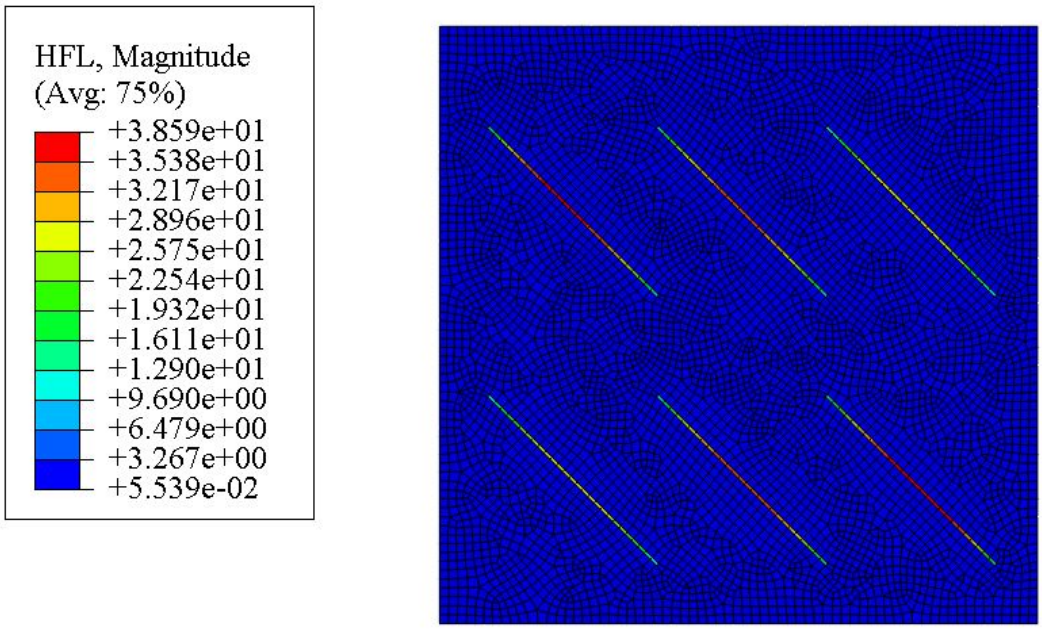

Figure 3.11: Heat flux plot for 2D platelets oriented at 45 °

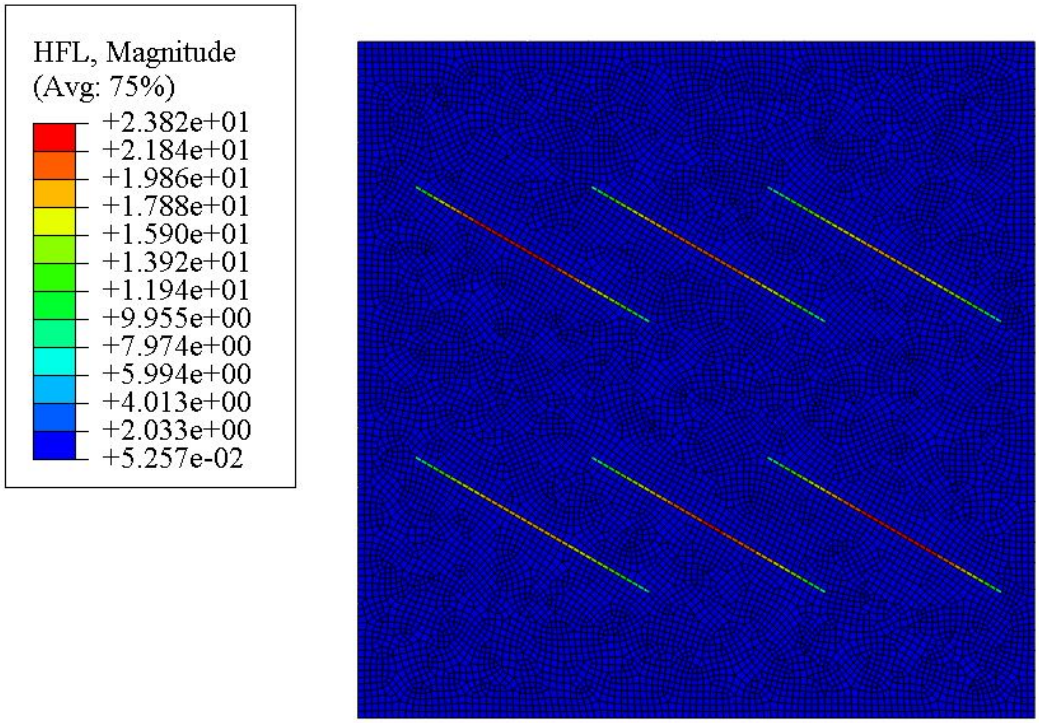

Figure 3.12: Heat flux plot for 2D platelets oriented at 60 °

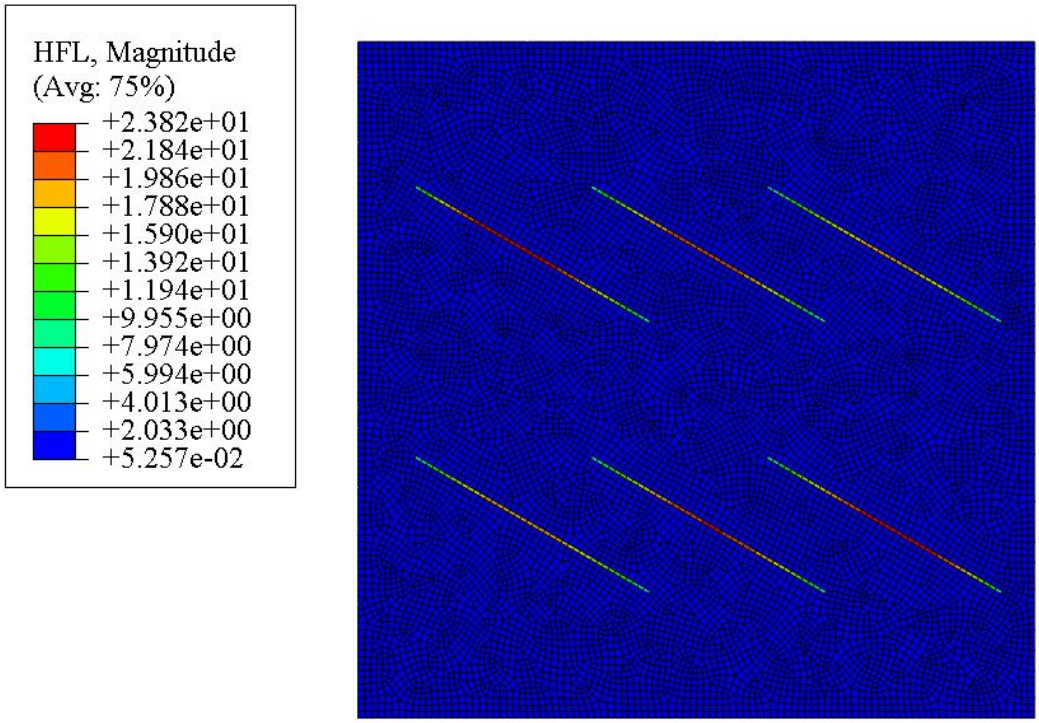

Figure 3.13: Heat flux plot for 2D platelets oriented at 75 °

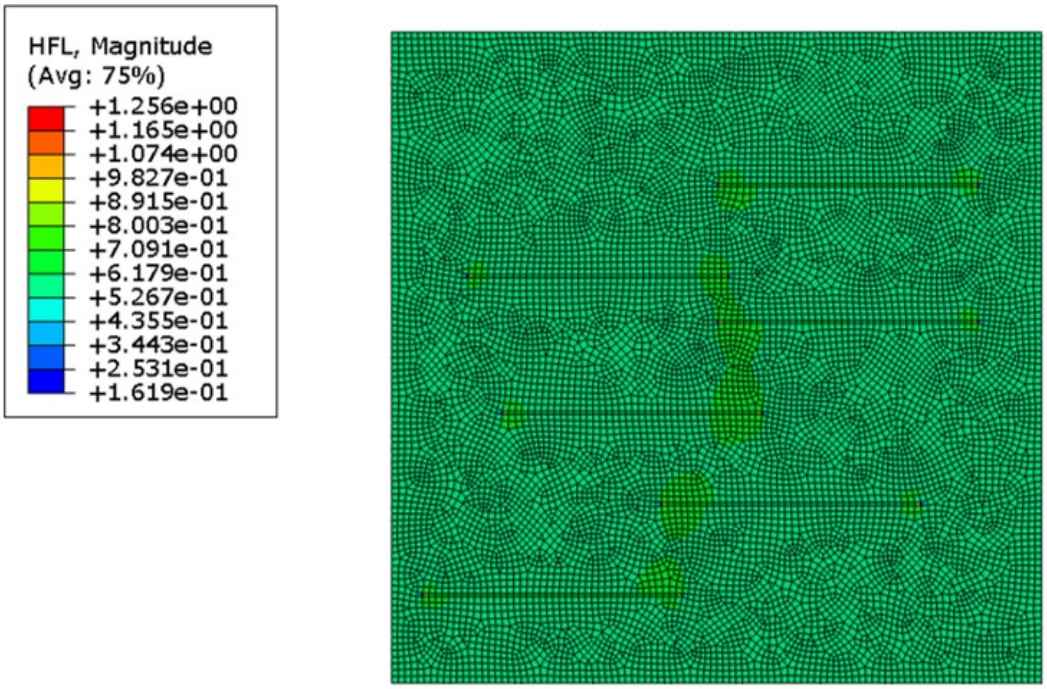

Figure 3.14: Heat flux plot for 2D platelets oriented at 90°

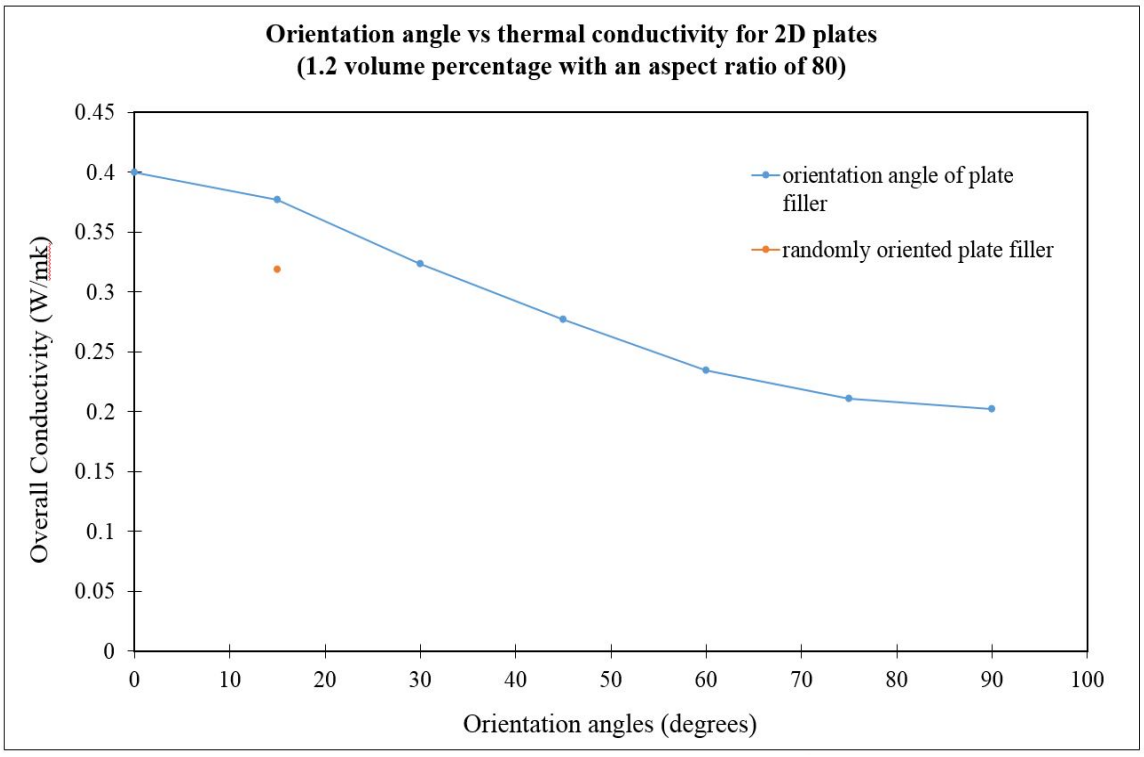

Figure 3.15: Overall conductivity vs Orientation angle (2D platelets)

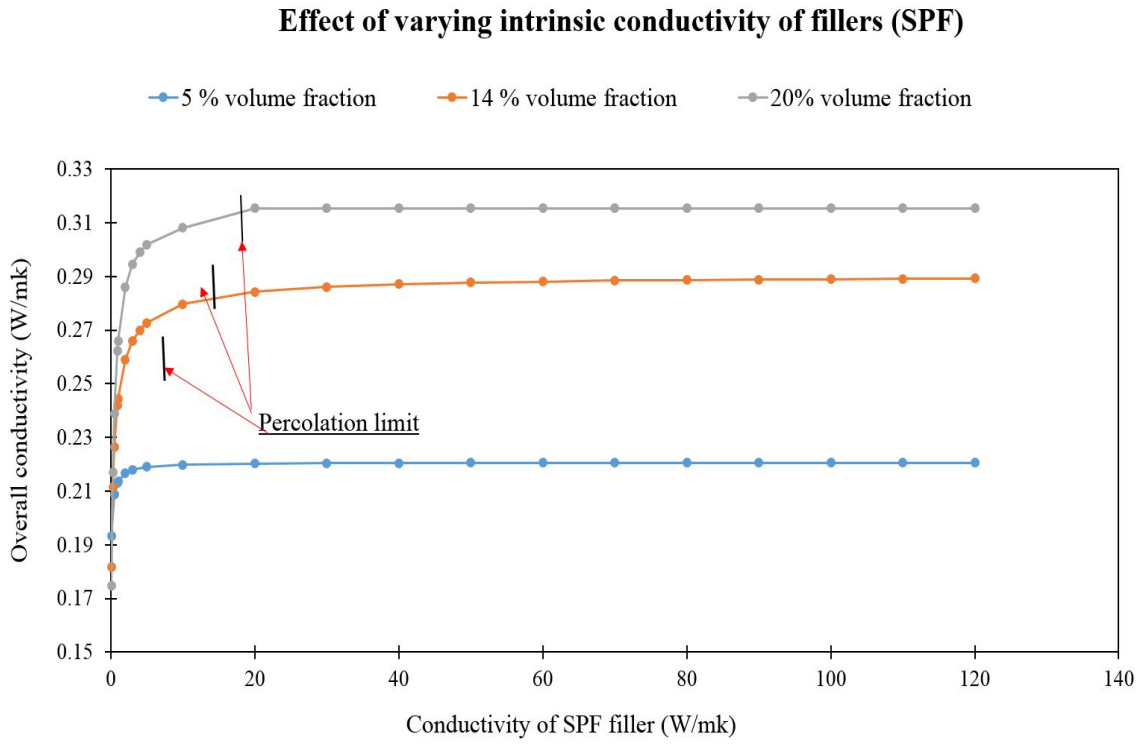

Figure 3.16: Overall conductivity vs intrinsic conductivity of filler

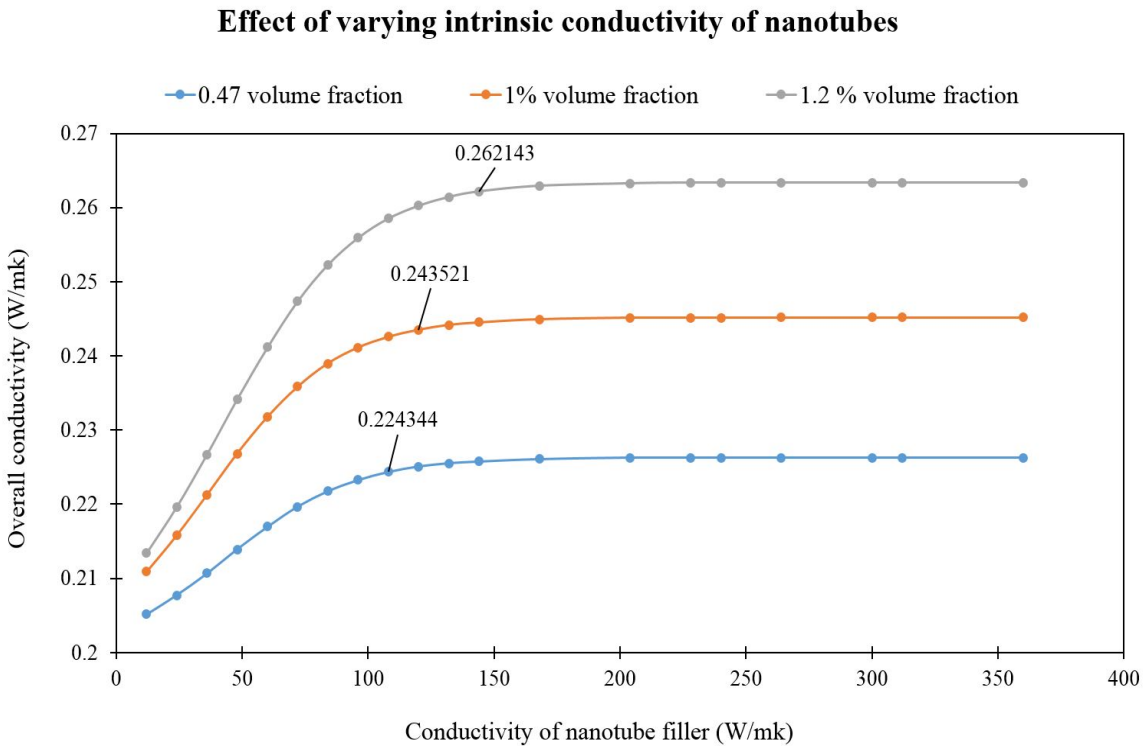

Figure 3.17: Overall conductivity vs intrinsic conductivity of filler (3D CNT)

CHAPTER 4: FEM COMPARISON WITH HOMOGENIZATION METHODS

4.1 Mean field Homogenization

In the last decade, and before that, numerous models are proposed to effectively determine the overall thermal conductivity of composites with fillers of different volume fractions. The theories developed are termed as effective medium approximation theories. As, it will be discussed further that due to their nature and approximations used while developing these theories, they are unable to effectively determine the the overall properties of heterogeneous materials beyond a certain volume fraction or percolation threshold. In this section, the concept and general ingredients of homogenization methods are discussed [15].

Homogenization refers to the idea of making uniform, the properties of inhomogeneous or heterogeneous materials to get a good approximation. As discussed in the introduction section, modeling domain represents the micro structure of the material just like an integration point in the finite element software.

In this method the results are computed on the imaginary modeling domain and returned to the macro-scale by using averaging techniques. Since a detailed analysis of strains and stresses are computed on the modeling domain, it can be seen as a very accurate method.

The fillers aka inclusions aka inhomogeneities are considered as separate homogeneous entities or domains and the fields are represented by their averaged values. Scale transition which is the main steps in homogenization requires a smooth transition of macroscopic quantities to microscopic scales and vice-versa [16].

Averaging property is defined as [17]

$$[g(x)]_\omega = \frac{1}{V}\int_\omega g(x)dV = \bar{g} \tag{4.1}$$

where, $\bar{g}$ is the macroscopic value, g is any field over the domain, $[g(x)]_\omega$ is the averaged value of g over x coordinates on volume ω

Equation 2.3 can now be decomposed into sub domains, and can be written as,[17]

$$[g(x)]_\omega = \frac{1}{V}\sum_k \int_{\omega_k} g(x)dV_k \tag{4.2}$$

Equation 2.4 can be written in terms of volume fraction, and is given by, [17]

$$[g(x)]_\omega = \sum_k f_k g(x)_{\omega_k} \tag{4.3}$$

where, f is the volume fraction, and is given by,[17]

$$f_k = \frac{V_k}{V} \tag{4.4}$$

where, V_k is the volume of sub-domain and V is the total volume.

Some of the assumptions in Mean field homogenization theories are described here [18],

1) It is possible to describe macroscopic quantities with averages of microscopic quantities.

2) Interaction effects of different phases are neglected.

3) In a particular phase the macroscopic behavior is same throughout the microstructure.

Eshelby introduced a method to find the temperature gradient concentration tensor which is known as the Inclusion theory. By Using superposition principle of elasticity and Greens function, Eshelby was able to derive a relation between the eigen

temperature tensor and the constrained temperature tensor and is given by, [19]

$$t^c_{ij} = S_{ijkl} t^*_{kl} \tag{4.5}$$

where S_{ijkl} is Eshelby's tensor, t^c_{ij} is the constrained temperature gradient tensor, and t^*_{kl} is the eigen temperature gradient tensor.

Eshelby's tensor satisfy minor symmetries but not major symmetries. Mathematically it is written as, '

$$S_{ijkl} = S_{jikl} = S_{ijlk} \tag{4.6}$$

In essence, Eshelby's tensor is a function of space but a result obtained by eshelby is that For an ellipsoidal or spherical inclusion eshelby's tensor is constant. Also, explicit expressions of Eshelby's tensor can be derived for various filler geometries such as prolate and oblate shaped. These expressions are shown discussed in the following subsections.

4.1.1 Mori-Tanaka Homogenization

For a two phase composite material, Mori and Tanaka developed an approximation theory which is based on mean field micro-mechanics method. In this it estimates the average filler tensor field subjected to overall tensor field. This method is applicable for low volume fractions or very high volume fractions.

$$A^m_{MT} = [(1 - v_f)I + A^i_{dil}]^{-1} \tag{4.7}$$

$$A^i_{MT} = A^i_{dil}[(1 - v_f)I + A^i_{dil}]^{-1} \tag{4.8}$$

$$A^i_{dil} = [I + S \cdot (K^m)^{-1} \cdot (K^i - K^m)]^{-1} \tag{4.9}$$

where subscripts *dil* and MT stands for inclusion dilute and Mori-Tanaka matrices, superscripts 'i' and 'm' stands for inclusion and matrix respectively

For spherical fillers, Eshelby's tensor is given by,

$$S_{11} = S_{22} = S_{33} = \frac{1}{3} \tag{4.10}$$

For cylindrical fillers, Eshelby's tensor is given by,

$$S_{11} = S_{22} = \frac{a_1^2 a_3}{2(a_3^2 - a_1^2)^{3/2}} \left(\frac{a_3}{a_1} \left(\frac{a_3^2}{a_1^2} - 1 \right)^{1/2} - cosh^{-1} \frac{a_3}{a_1} \right) \tag{4.11}$$

$$S_{33} = 1 - 2S_{22} \tag{4.12}$$

4.1.2 Maxwell-Garnett Effective medium Approximation

Hasselman and Johnson [20] extended the work of Maxwell and derived the MG-EMA for spherical and cylindrical type of fillers. This method is based on scattering theory of waves and particles [21]. Nan [22] extended the work and derived the equations to find the effective thermal conductivity of fillers with randomly dispersed and oriented fillers and is given by,

Effective conductivity for spherical fillers, [23]

$$K^* = K_m \frac{2f(K_i - K_m) + K_i + 2K_m}{2K_m + K_i + f(K_m - K_i)} \tag{4.13}$$

Effective conductivity for cylindrical or plate type fillers, [17]

$$K^* = K_m \frac{3 + f[2\beta_{11}(1 - L_{11}) + \beta_{33}(1 - L_{33})]}{3 - f[2\beta_{11}L_{11} + \beta_{33}L_{33}]} \tag{4.14}$$

where K^* is the Overall thermal conductivity, K_m is the conductivity of matrix,K_i is the thermal conductivity of inclusion, f is the volume fraction and L_{ii} is the geo-

metrical factor and it depends on the shape of the geometry

for cylindrical fillers,

$$L_{11} = L_{22} = \frac{p^2}{2(p^2-1)} - \frac{p}{2(p^2-1)^{1.5}} \cosh^{-1}(p) \tag{4.15}$$

where p is the aspect ratio and is given by $p = \frac{a_1}{a_3}$; a_1 and a_3 are the radii of two perpendicular axes of filler, also $p > 1$ for cylindrical fillers

for plate type fillers,

$$L_{11} = L_{22} = \frac{p^2}{2(p^2-1)} - \frac{p}{2(p^2-1)^{1.5}} \cos^{-1}(p) \tag{4.16}$$

$p < 1$ for plate like fillers

$$L_{33} = 1 - 2L_{11} \tag{4.17}$$

The parameter β_{ii} is given by,

$$\beta_{ii} = \frac{K_{ii}^c - K_m}{K_m + L_{ii}(K_{ii}^c - K_m)} \tag{4.18}$$

the equivalent thermal conductivity K_{ii}^c is given by,

$$K_{ii}^c = \frac{K_i}{(1 + \gamma L_{ii} \frac{K_i}{K_m})} \tag{4.19}$$

It is showed by Dunn and Taya that the Maxwell-Garnett effective medium approximation becomes inaccurate as the volume fraction is increased after a certain percentage. Therefore one part of the present study also shows that there is a need of more elaborate methods to effectively determine the thermal conductivity of composite.

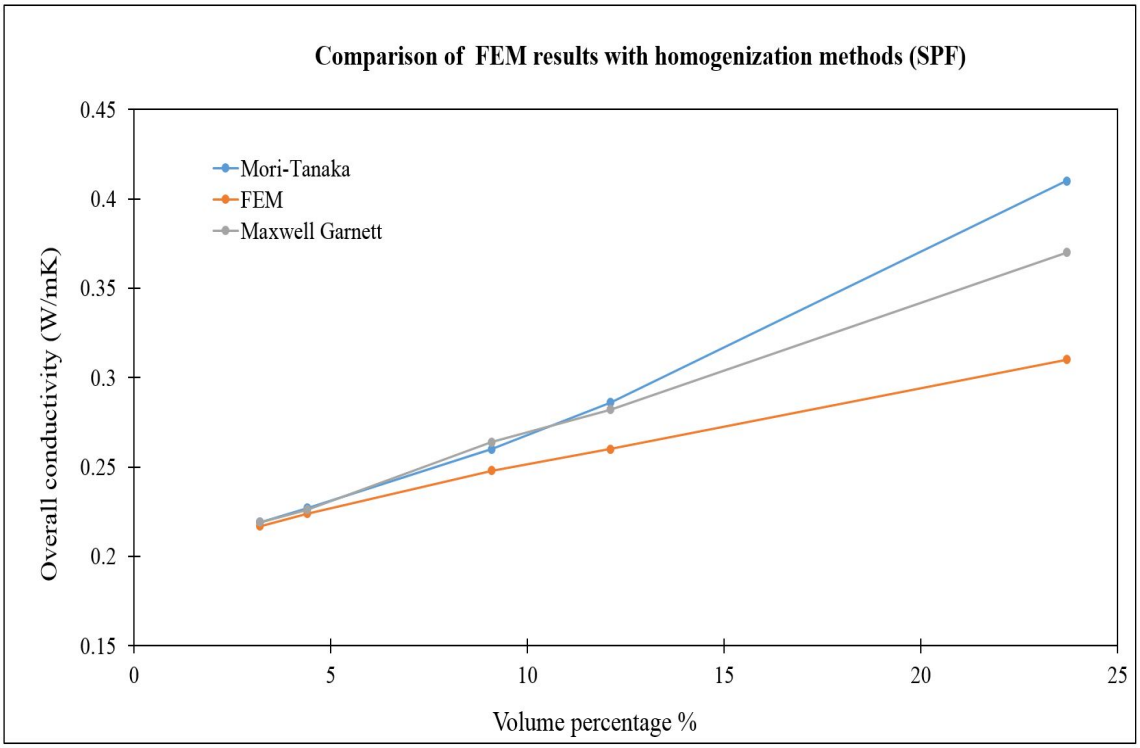

Figure 4.1: Result validation for 3D SPF

4.2 FEM, Mori-Tanaka and Maxwell Garnett effective medium approximation for SPF

The results of finite element method are validated with two of the most important homogenization methods i.e Mori-Tanaka and Maxwell Garnett effective medium approximation. The theory and formulas described in the previous sections are used to derive the values of thermal conductivity at a particular volume fraction. A matlab program is written which takes into account the formulas and displays the result of effective conductivity. The comparison of FEM, Mori-Tanaka and Maxwell Garnett approximations. The figure 4.1 shows the comparison of homogenization methods with FEM with overall conductivity on y-axis and volume percentage on x-axis.

It can be seen that the Mori-Tanaka and Maxwell Garnett agree with each other when the volume fraction is low i.e around 10% in the present case. When the volume fraction is increased further, the trends start to diverge away from each other.

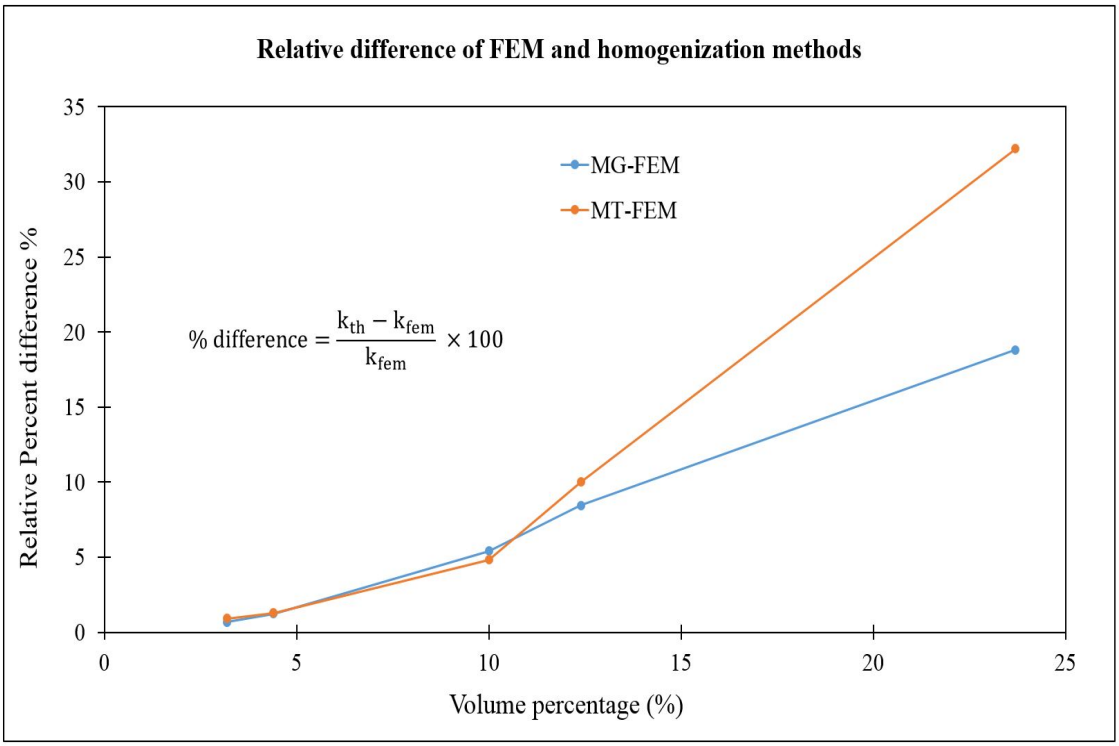

Figure 4.2: Relative percentage difference vs volume percentage

Figure 4.2 shows the relative percentage difference graph against volume fraction. The percentage difference is calculated by,

$$\% \text{ difference} = \frac{k_{\text{theoretical}} - k_{\text{fem}}}{k_{\text{fem}}} \times 100 \tag{4.20}$$

4.3 FEM and Mori-Tanaka for CNT

In order to see how the increasing volume percentage affects the overall conductivity in case of carbon nano-tubes for FEM and Mori-Tanaka an analysis is performed where the aspect ratio of carbon nano-tubes are kept constant and the volume percentage is varied. The results show that the FEM and Mori-Tanaka results agree at lower volume percentages but at higher volume percentages the relative percentage error is more. Figure 4.3 shows the graph of conductivity vs volume percentage of fillers and Figure 4.4 shows the relative percentage difference graph vs the volume percentage.

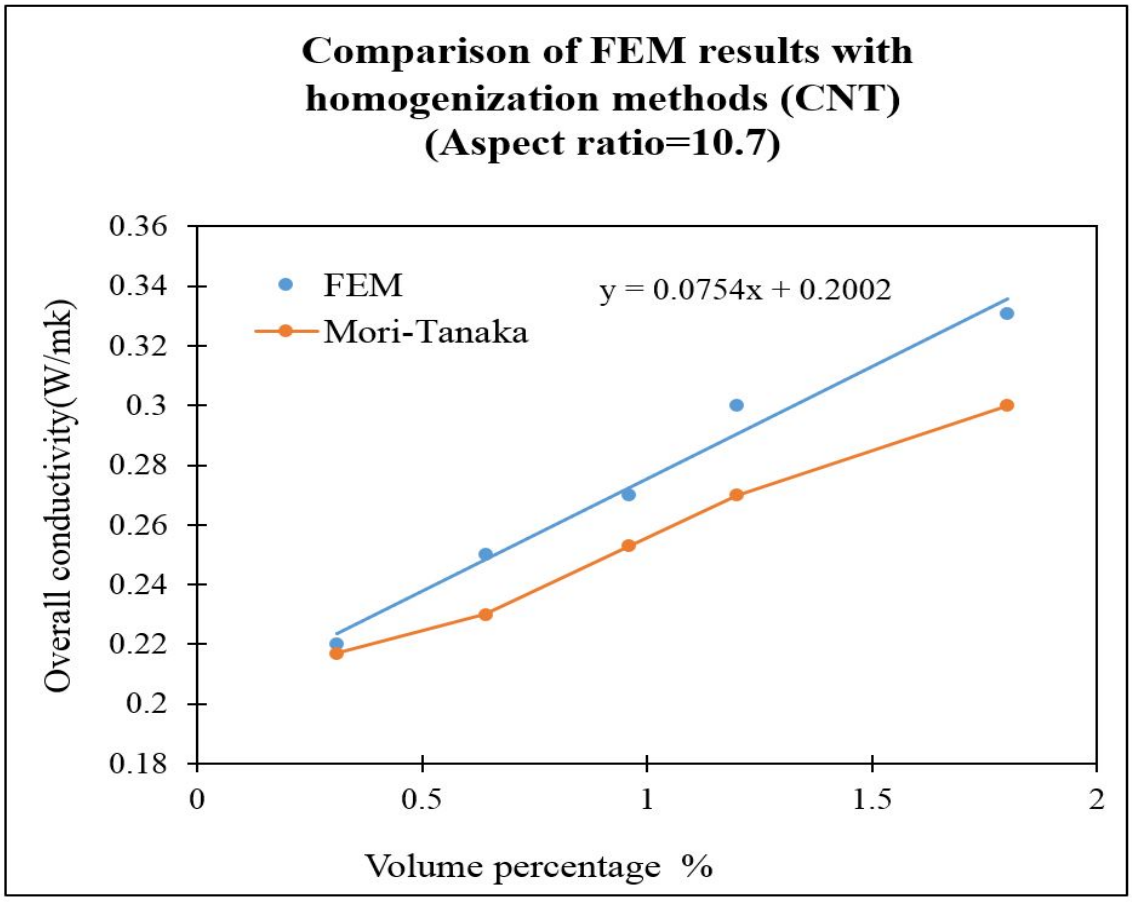

Figure 4.3: CNT result validation

The FEM results are compared with analytical homogenization methods Mori-Tanaka and Maxwell-Garnett effective medium approximation with some limitations. Since the theoretical methods stands on a lot of assumptions, they are well suited for low filler volume fractions and becomes highly inaccurate for higher filler volume fractions. Therefore one part of the study also highlights the need for improving the homogenization methods in order to reliably predict the heat transfer in composites.

Therefore our 3D finite element model reveals that the mean field homogenization methods are not very accurate and reliable approaches to effectively predict the overall thermal conductivity of composites specially at higher volume fractions.

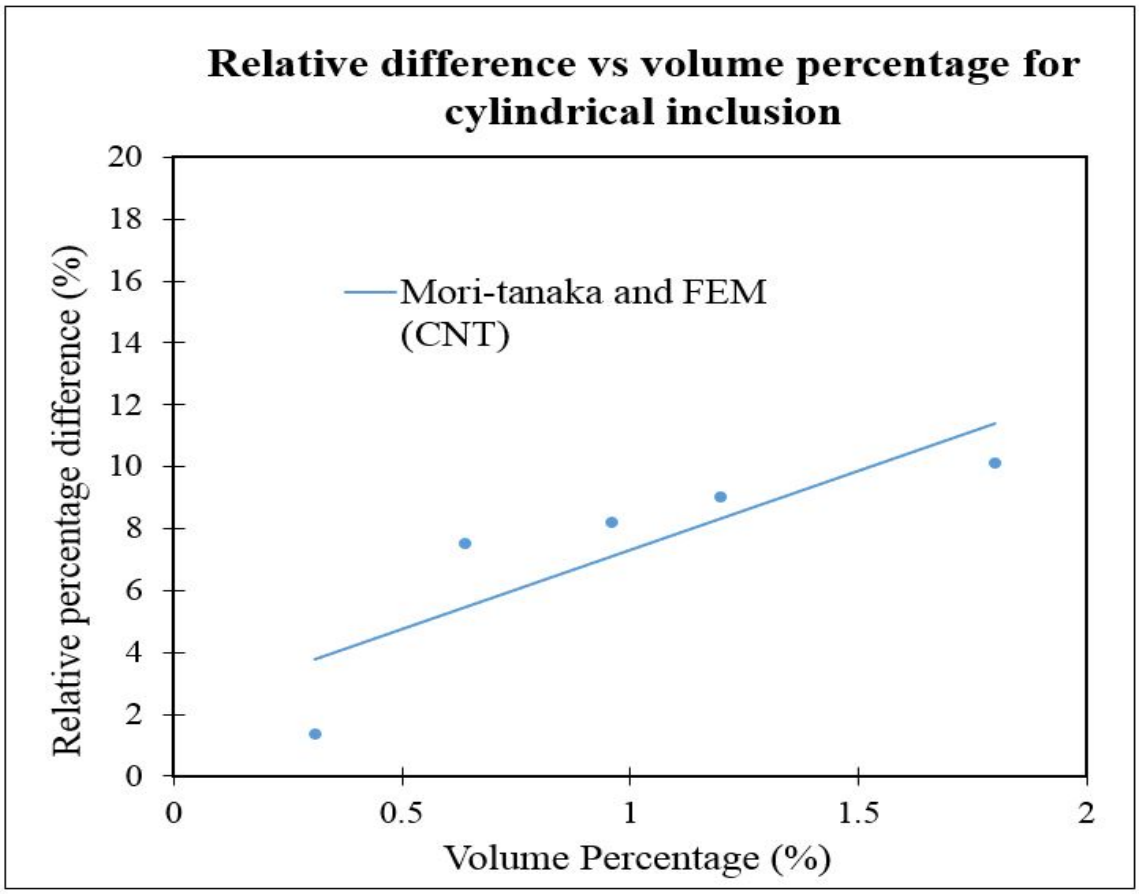

Figure 4.4: Relative percentage difference vs volume percentage for 3D CNT

CHAPTER 5: CONCLUSIONS

1) 2D and 3D FEM models were developed and analyzed in the present study.

2) Filler properties such as shape, size and aspect ratio of the fillers were varied and their effect on the Composite was found.

3) Orientation angle and aspect ratio have a significant effect on the overall thermal conductivity of rubber composites.

4) Thermal conductivity increased with increasing aspect ratio of the carbon nanotubes because of higher surface to volume ratio and more availability of were for heat transfer.

5) Thermal conductivity decreased with increasing orientation angle, and when the orientation of filer was in the direction perpendicular to the heat flux, the overall thermal conductivity was at minimum.

6) FEM results were validated with analytical homogenization methods at lower volume fractions and found that for higher volume fractions, the results significantly deviate.

7) The relative percent difference error for MG-FEM and MT-FEM significantly increased after 10% volume fraction.

8) It is concluded that the analysis can be used as a tool to tailor the thermal properties of ESBR matrix and fabricate the composite for required thermal conductivity. The analysis can also be used as an optimization tool and gain an insight into understanding the thermal behavior of composite materials.

REFERENCES

[1] Z. Li, W. Wu, H. Chen, Z. Zhu, Y. Wang, and Y. Zhang, "Thermal conductivity of micro/nano filler filled polymeric composites," *RSC Advances*, vol. 3, no. 18, p. 6417, 2013.

[2] C. Huet, "Application of variational concepts to size effects in elastic heterogeneous bodies," *Journal of the Mechanics and Physics of Solids*, vol. 38, pp. 813–841, jan 1990.

[3] A. Almasi, M. Silani, H. Talebi, and T. Rabczuk, "Stochastic analysis of the interphase effects on the mechanical properties of clay/epoxy nanocomposites," *Composite Structures*, vol. 133, pp. 1302–1312, dec 2015.

[4] C. Sun and R. Vaidya, "Prediction of composite properties from a representative volume element," *Composites Science and Technology*, vol. 56, pp. 171–179, jan 1996.

[5] P. Wendt, "The control of rubber in world war II," *Southern Economic Journal*, vol. 13, p. 203, jan 1947.

[6] X. Wang, Q. Li, J. Xie, Z. Jin, J. Wang, Y. Li, K. Jiang, and S. Fan, "Fabrication of ultralong and electrically uniform single-walled carbon nanotubes on clean substrates," *Nano Letters*, vol. 9, pp. 3137–3141, sep 2009.

[7] S. D. Pilla, *Slip and Fall Prevention: A Practical Handbook*. CRC Press, 2004.

[8] G. D. Seidel and D. C. Lagoudas, "A micromechanics model for the thermal conductivity of nanotube-polymer nanocomposites," *Journal of Applied Mechanics*, vol. 75, no. 4, p. 041025, 2008.

[9] "The a to z of materials."

[10] R. S. Amit Devpura, Patrick E. Phelan, "SIZE EFFECTS ON THE THERMAL CONDUCTIVITY OF POLYMERS LADEN WITH HIGHLY CONDUCTIVE FILLER PARTICLES," *Microscale Thermophysical Engineering*, vol. 5, pp. 177–189, jul 2001.

[11] R. Hill, "Elastic properties of reinforced solids: Some theoretical principles," *Journal of the Mechanics and Physics of Solids*, vol. 11, pp. 357–372, sep 1963.

[12] W. Drugan and J. Willis, "A micromechanics-based nonlocal constitutive equation and estimates of representative volume element size for elastic composites," *Journal of the Mechanics and Physics of Solids*, vol. 44, pp. 497–524, apr 1996.

[13] *Abaqus user's manual*.

[14] J. R. Cannon, *The One-Dimensional Heat Equation (Encyclopedia of Mathematics and its Applications)*. Cambridge University Press, 1984.

[15] D. Ganapathy, K. Singh, P. E. Phelan, and R. Prasher, "An effective unit cell approach to compute the thermal conductivity of composites with cylindrical particles," *Journal of Heat Transfer*, vol. 127, no. 6, p. 553, 2005.

[16] A. E. Moumen, T. Kanit, A. Imad, and H. E. Minor, "Effect of reinforcement shape on physical properties and representative volume element of particles-reinforced composites: Statistical and numerical approaches," *Mechanics of Materials*, vol. 83, pp. 1–16, apr 2015.

[17] B. He, B. Mortazavi, X. Zhuang, and T. Rabczuk, "Modeling kapitza resistance of two-phase composite material," *Composite Structures*, vol. 152, pp. 939–946, sep 2016.

[18] H. Hiroshi and T. Minoru, "Equivalent inclusion method for steady state heat conduction in composites," *International Journal of Engineering Science*, vol. 24, pp. 1159–1172, jan 1986.

[19] W. J. Parnell, *The Hill and Eshelby tensors for ellipsoidal inhomogeneities in the Newtonian potential problem and linear elastostatics*.

[20] T. Kanit, S. Forest, I. Galliet, V. Mounoury, and D. Jeulin, "Determination of the size of the representative volume element for random composites: statistical and numerical approach," *International Journal of Solids and Structures*, vol. 40, pp. 3647–3679, jun 2003.

[21] W. Cai and V. Shalaev, *Optical Metamaterials: Fundamentals and Applications*. Springer, 2009.

[22] C.-W. Nan, R. Birringer, D. R. Clarke, and H. Gleiter, "Effective thermal conductivity of particulate composites with interfacial thermal resistance," *Journal of Applied Physics*, vol. 81, pp. 6692–6699, may 1997.

[23] O. Levy and D. Stroud, "Maxwell garnett theory for mixtures of anisotropic inclusions: Application to conducting polymers," *Physical Review B*, vol. 56, pp. 8035–8046, oct 1997.